**ELECTRONIC SUPPLEMENTARY INFORMATION**

# On the reduction of $CO_2$ footprint via selective hydrodeoxygenation by ZnO-$Ti_3C_2T_x$ catalyst under solvent-free conditions

Bhagirath Saini[a], R. Krishnapriya [b], Meena Yadav[a] Rahul Singhal[c], Rakesh K Sharma[a]*

[a]Sustainable Materials and Catalysis Research Laboratory (SMCRL), Department of Chemistry, Indian Institute of Technology Jodhpur, NH 65, Karwar, Jodhpur, Rajasthan, India, 342037 Tel.: +91 291 280 1303, E-mail: rks@iitj.ac.in

[b] Mechanical and Aerospace Engineering Department, College of Engineering, United Arab Emirate University, Al Ain 15551, UAE

[c]Department of Physics and Engineering Physics, Central Connecticut State University, New Britain, CT 06050, USA

**TABLE OF CONTENTS**

| | |
|---|---|
| Figure S42-S45 | HRMS, $^{1}H$ and $^{13}C$ NMR spec4tra of hydrotreatment reaction. |
| Figure S47-49 | XRD, EDX elemental mapping and SEM image after the hydrotreatment process of $Ti_3C_2T_x$ and ZnO-$Ti_3C_2T_x$nanocomposite. |
| Figure S50 | $^{1}H$ NMR of hydrotreatment reaction with time-dependent study. |
| Figure S51 | (a) GC chromatogram of hydrotreatment reaction with time-dependent study; (b-c) Conversation and selectivity data of Entry 9 at 4, 8 and 13h. |
| Table S1 | Comparative study of MXene and MXene-ZnO catalyst with previously reported study. |

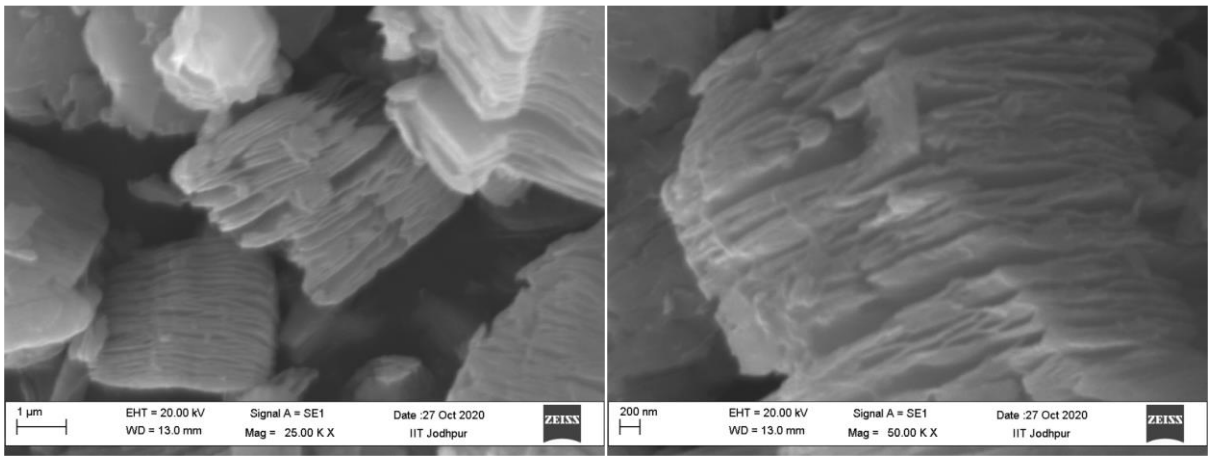


Figure S1: High magnification SEM images of MXene catalyst at 1µm and 200nm.

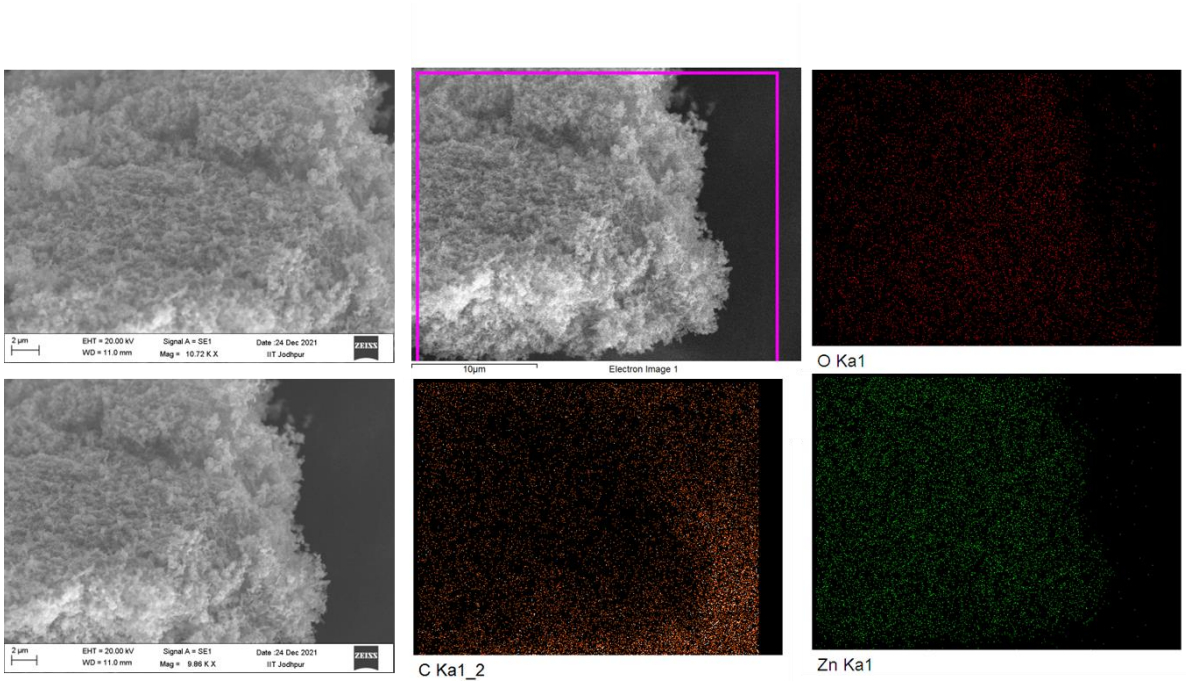


**Figure S2:** SEM image and EDX elemental mapping of ZnO nanoflakes.

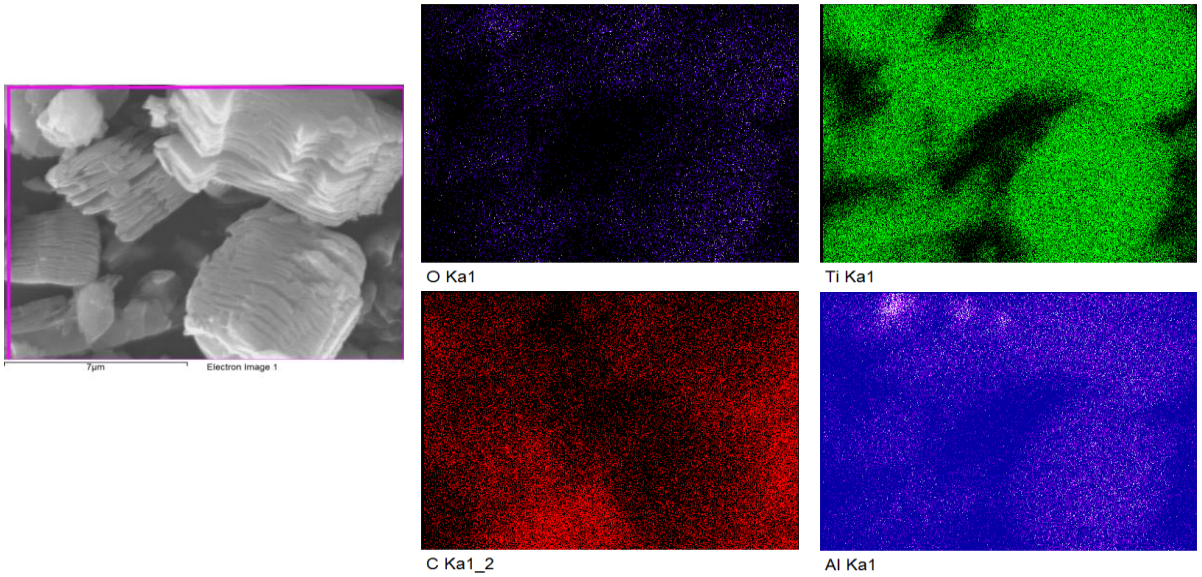


**Figure S3:** SEM image and EDX elemental mapping of $Ti_3C_2T_x$.

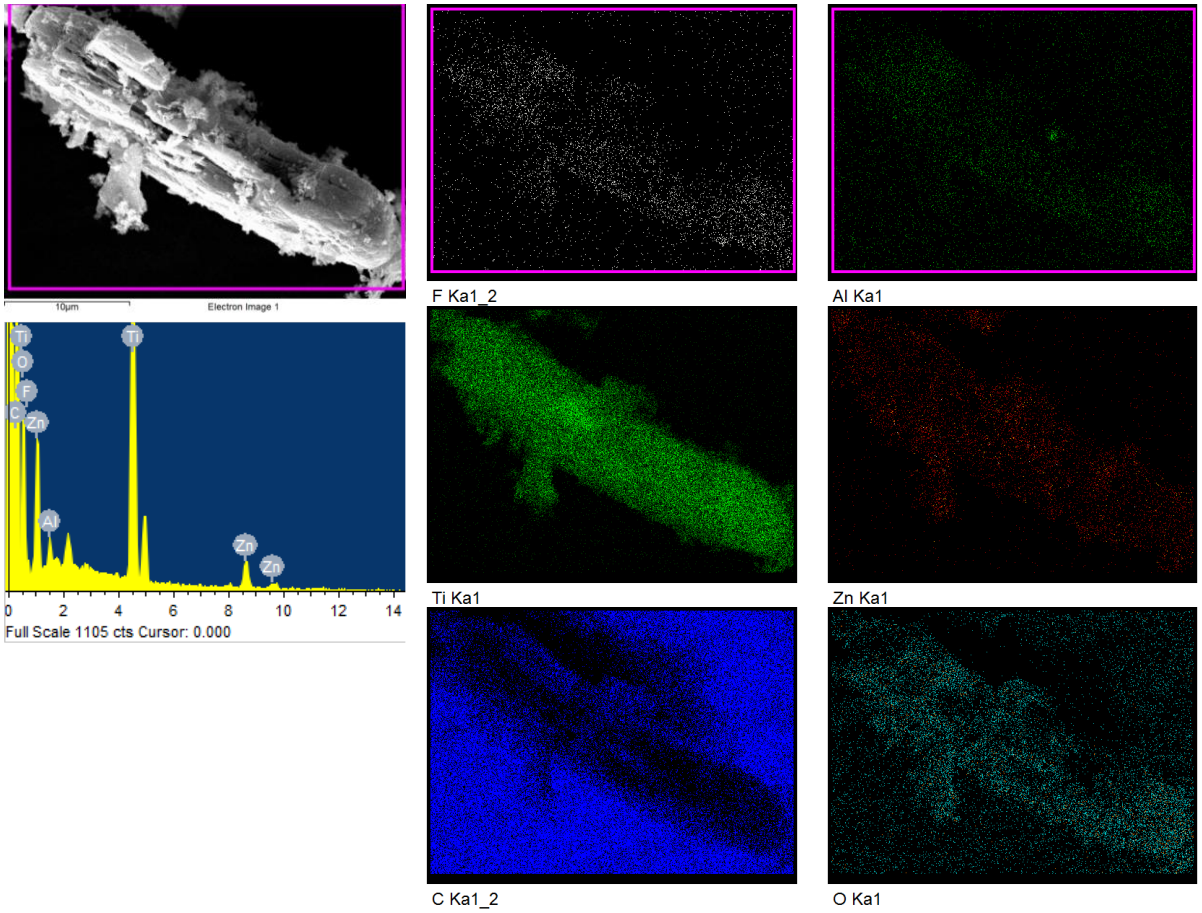


**Figure S4:** SEM image and EDX elemental mapping of ZnO-$Ti_3C_2T_x$ (15 wt%).

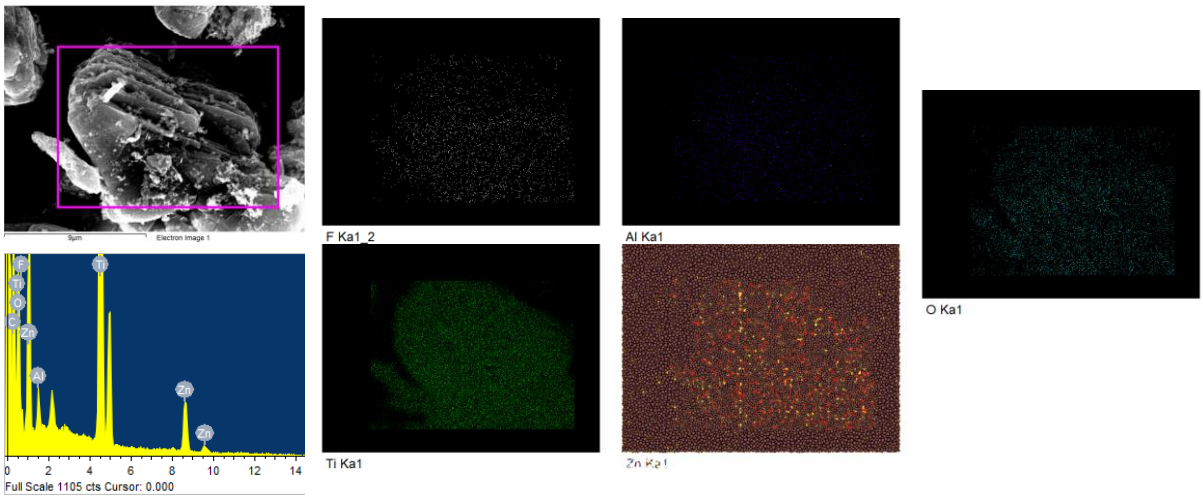


**Figure S5:** SEM image and EDX elemental mapping of ZnO-$Ti_3C_2T_x$ (10 wt%).

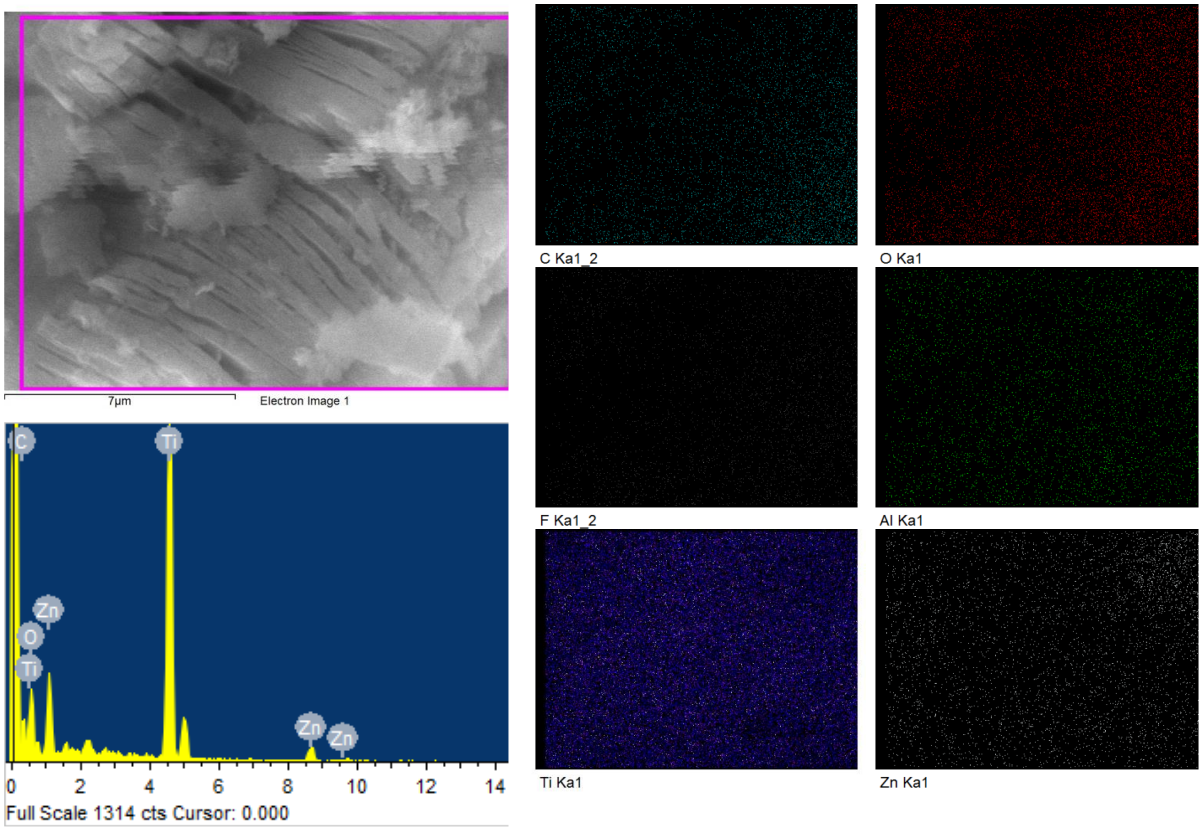


**Figure S6:** SEM image and EDX elemental mapping of ZnO-$Ti_3C_2T_x$ (5 wt%)

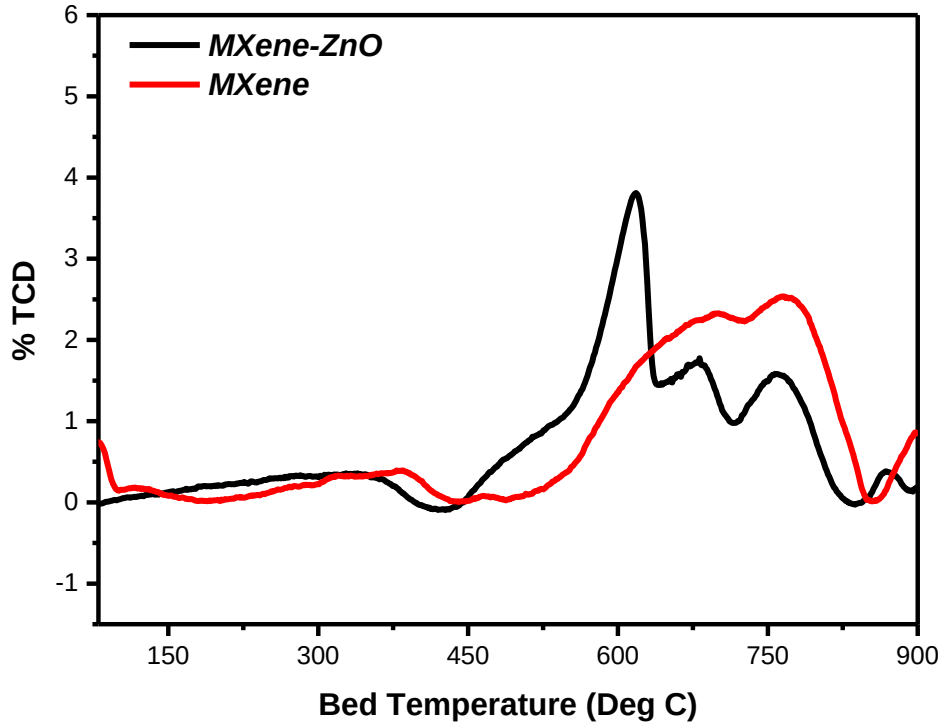


**Figure S7:** $NH_3$ TPD spectra of $Ti_3C_2T_x$, and ZnO-$Ti_3C_2T_x$ nanocomposite.

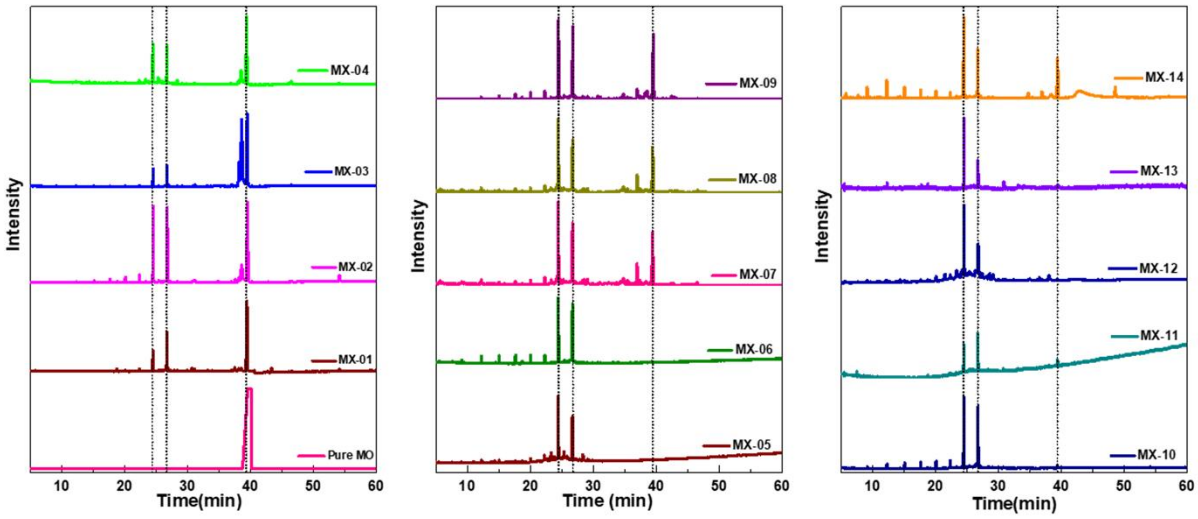


**Figure S8**. GC chromatogram of pure methyl oleate and for biodiesel product over $Ti_3C_2T_x$ catalyst, (a) pure methyl oleate and from MX-01 to MX-04, (b) MX-05 to MX-09, and (c) MX-10 to MX-14.

| Entry | Reaction | Code for graphs | Temp.(°C) | Pressure(B) | Time(Hr) | Solvent | Conversion (%) | Ratio (%) | |
|---|---|---|---|---|---|---|---|---|---|
| | | | | | | | | C17 | C18 |
| 1. | $Ti_3C_2$ | MX-01 | 200 | 20 | 08 | n- heptane | 36.02 | 10.44 | 25.58 |

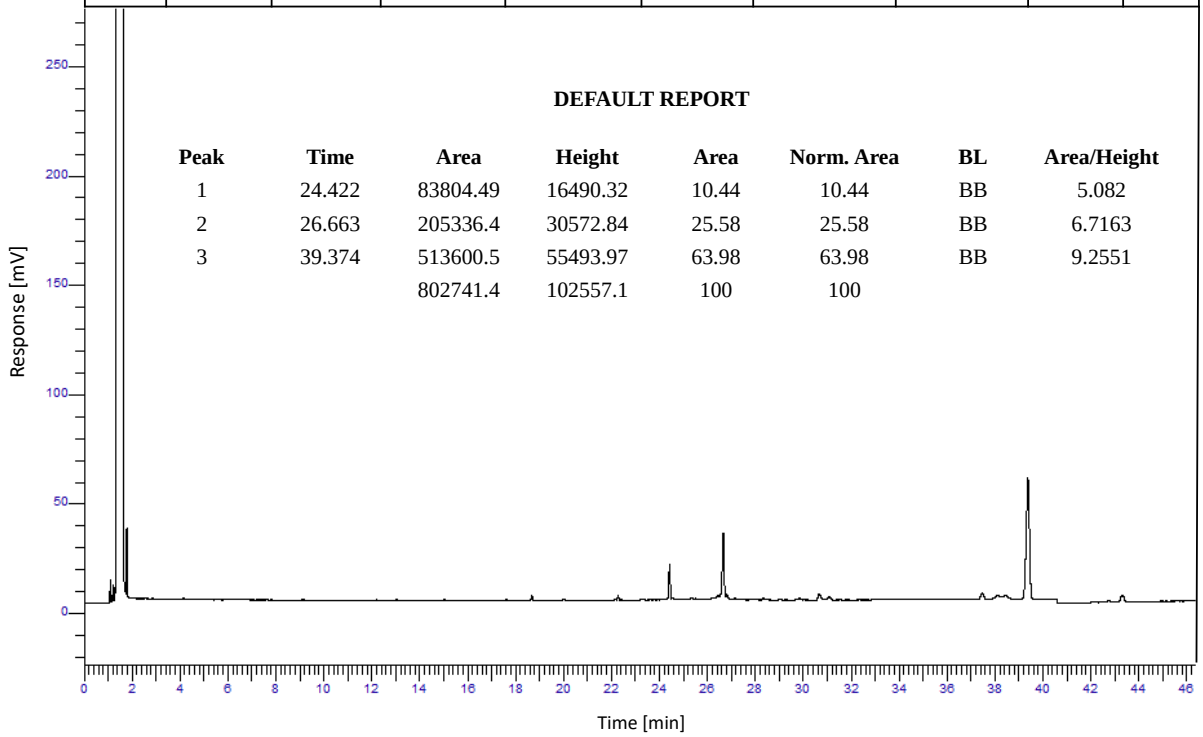


**Figure S9:** GC chromatogram for biodiesel product over $Ti_3C_2T_x$ catalyst (MX-01).

| Entry | Reaction | Code for graphs | Temp.(°C) | Pressure(B) | Time(Hr) | Solvent | Conversion (%) | Ratio (%) | |
|---|---|---|---|---|---|---|---|---|---|
| | | | | | | | | C17 | C18 |
| 2. | $Ti_3C_2$ | MX-02 | 250 | 20 | 08 | n- heptane | 56.79 | 19.17 | 26.69 |

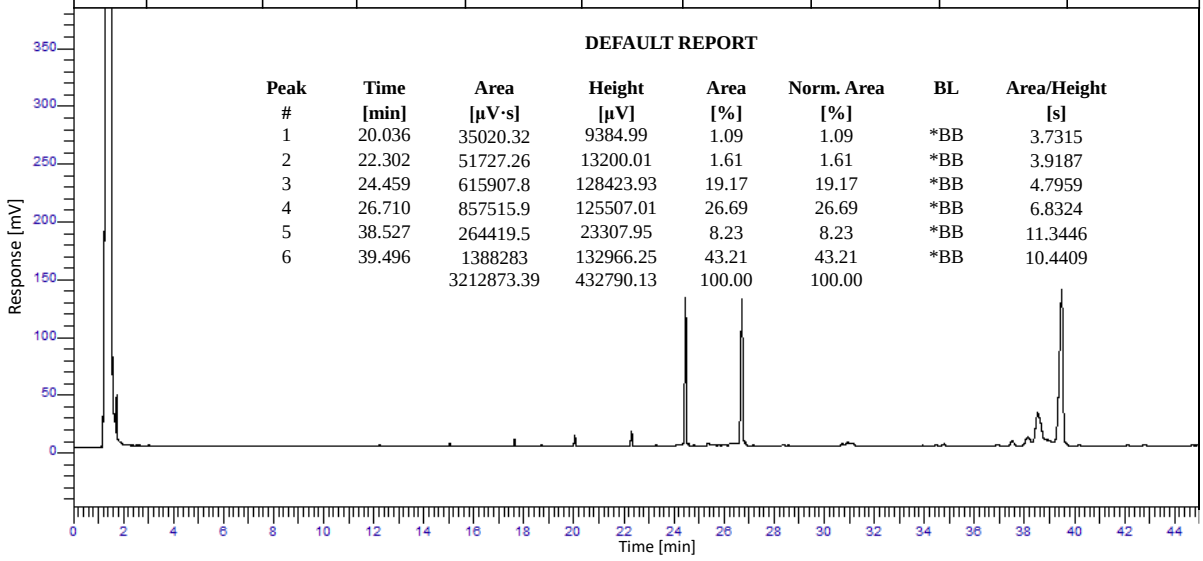


**Figure S10:** GC chromatogram for biodiesel product over $Ti_3C_2T_x$ catalyst (MX-02).

| Entry | Reaction | Code for graphs | Temp.(°C) | Pressure(B) | Time(Hr) | Solvent | Conversion (%) | Ratio (%) | |
|---|---|---|---|---|---|---|---|---|---|
| | | | | | | | | C17 | C18 |
| 3. | $Ti_3C_2$ | MX-03 | 250 | 30 | 08 | n- heptane | 58.76 | 6.23 | 7.12 |

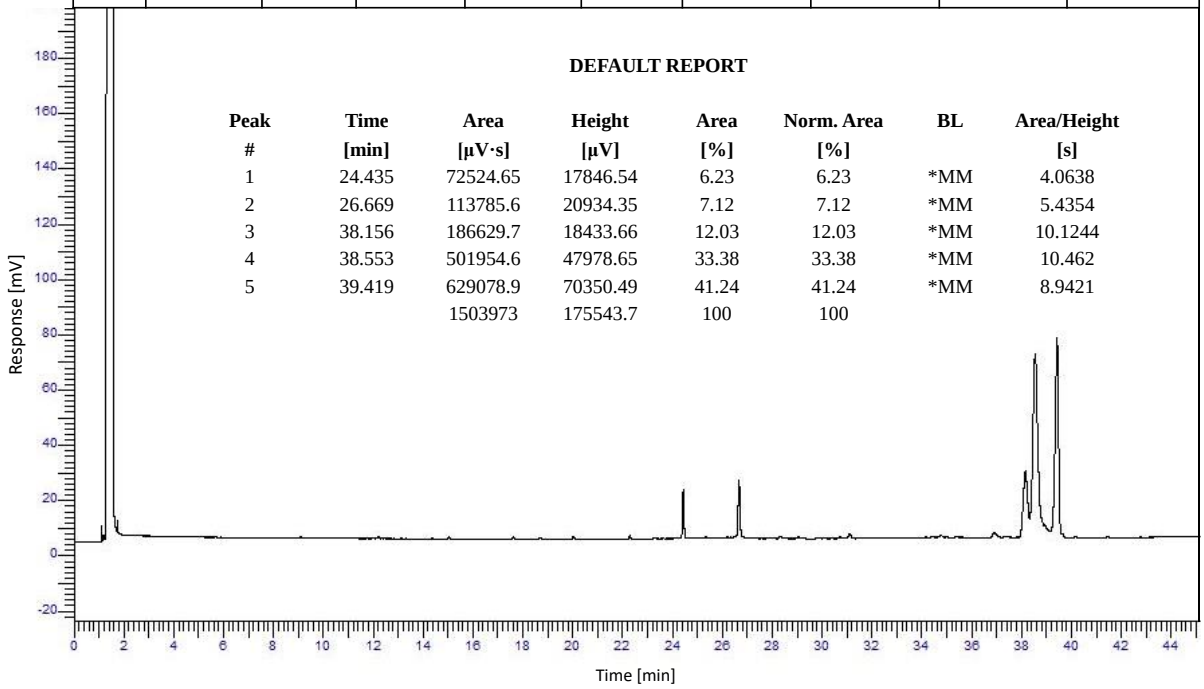


**Figure S11:** GC chromatogram for biodiesel product over $Ti_3C_2T_x$ catalyst (MX-03).

| Entry | Reaction | Code for graphs | Temp.(°C) | Pressure(B) | Time(Hr) | Solvent | Conversion (%) | Ratio (%) | |
|---|---|---|---|---|---|---|---|---|---|
| | | | | | | | | C17 | C18 |
| 4. | $Ti_3C_2$ | MX-04 | 280 | 30 | 08 | n- heptane | 63.77 | 23.57 | 24.19 |

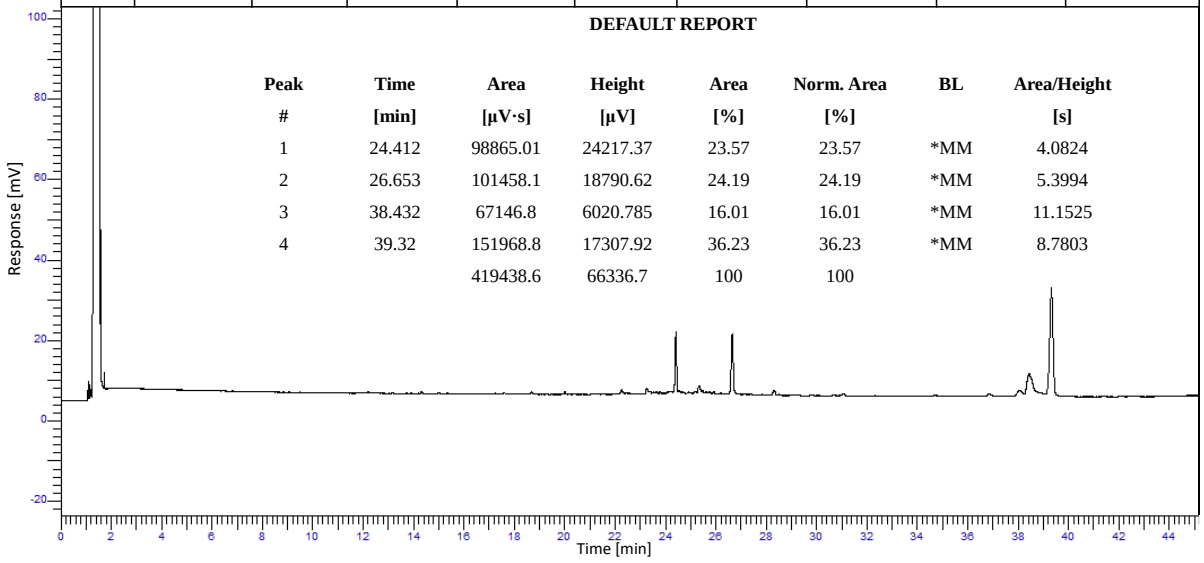


**Figure S12:** GC chromatogram for biodiesel product over $Ti_3C_2T_x$ catalyst (MX-04).

| Entry | Reaction | Code for graphs | Temp.(°C) | Pressure(B) | Time(Hr) | Solvent | Conversion (%) | Ratio (%) | |
|---|---|---|---|---|---|---|---|---|---|
| | | | | | | | | C17 | C18 |
| 5. | $Ti_3C_2$ | MX-05 | 280 | 30 | 12 | n- heptane | 100 | 47.14 | 41.25 |

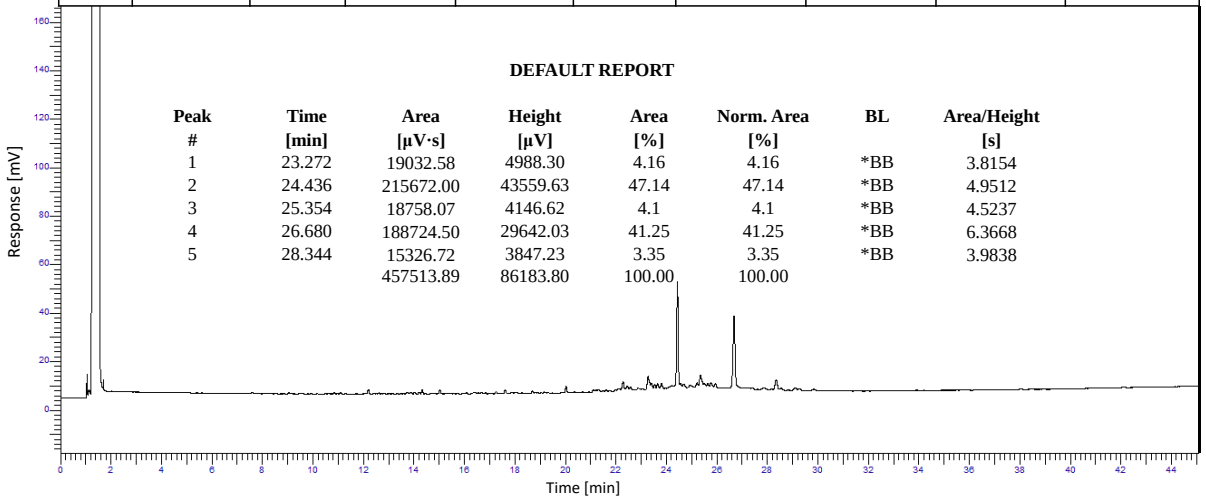


**Figure S13:** GC chromatogram for biodiesel product over $Ti_3C_2T_x$ catalyst (MX-05).

| Entry | Reaction | Code for graphs | Temp.(°C) | Pressure(B) | Time(Hr) | Solvent | Conversion (%) | Ratio (%) | |
|---|---|---|---|---|---|---|---|---|---|
| | | | | | | | | C17 | C18 |
| 6. | $Ti_3C_2$ | MX-06 | 320 | 30 | 12 | n- heptane | 100 | 34.39 | 45.51 |

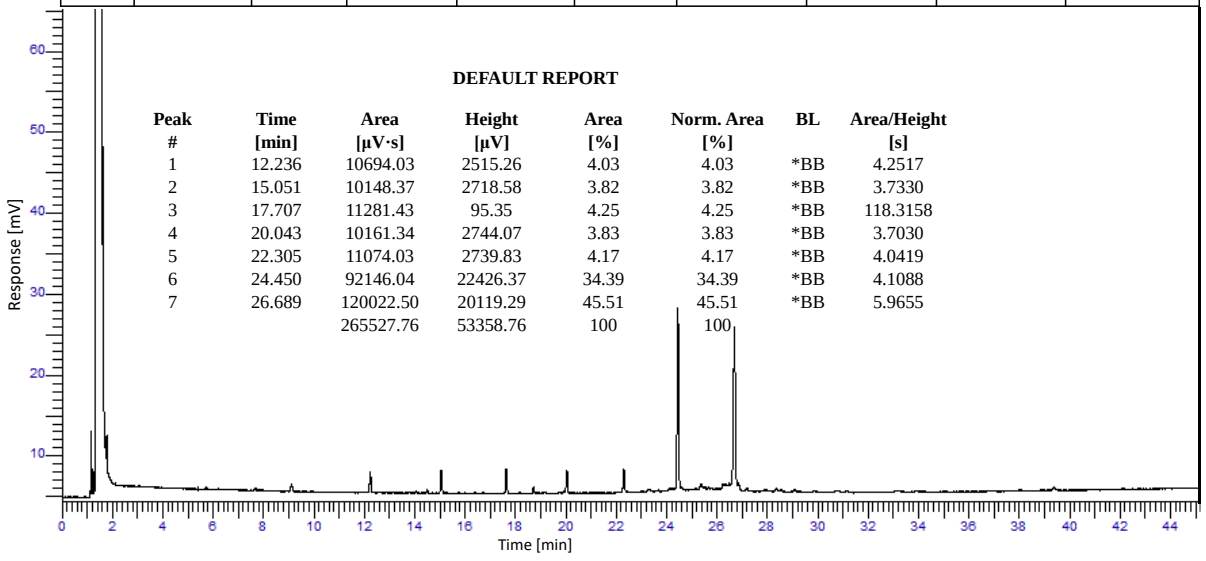


**Figure S14:** GC chromatogram for biodiesel product over $Ti_3C_2T_x$ catalyst (MX-06).

| Entry | Reaction | Code for graphs | Temp.(°C) | Pressure(B) | Time(Hr) | Solvent | Conversion (%) | Ratio (%) | |
|---|---|---|---|---|---|---|---|---|---|
| | | | | | | | | C17 | C18 |
| 7. | $Ti_3C_2$ | MX-07 | 320 | 30 | 12 | None | 70.7 | 33.24 | 27.21 |

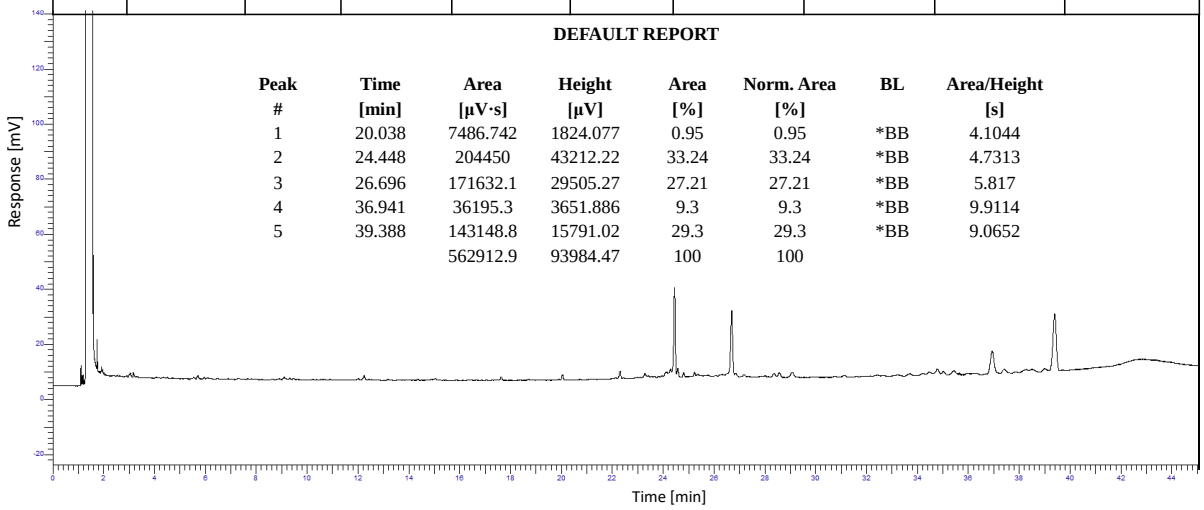


**Figure S15:** GC chromatogram for biodiesel product over $Ti_3C_2T_x$ catalyst (MX-07).

| Entry | Reaction | Code for graphs | Temp.(°C) | Pressure(B) | Time(Hr) | Solvent | Conversion (%) | Ratio (%) | |
|---|---|---|---|---|---|---|---|---|---|
| | | | | | | | | C17 | C18 |
| 8. | $Ti_3C_2$ | MX-08 | 280 | 30 | 12 | None | 66.63 | 28.65 | 23.98 |

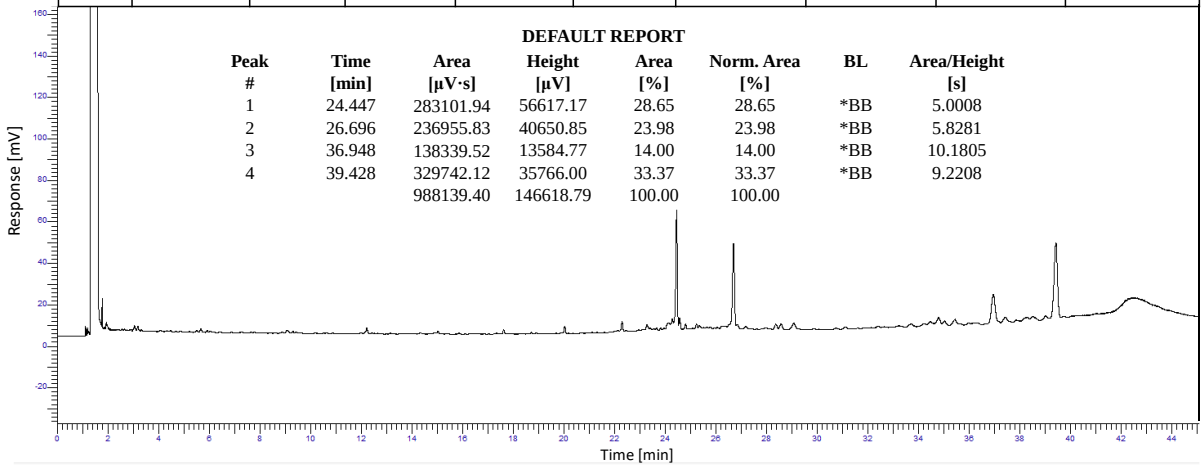


**Figure S16:** GC chromatogram for biodiesel product over $Ti_3C_2T_x$ catalyst (MX-08).

| Entry | Reaction | Code for graphs | Temp.(°C) | Pressure(B) | Time(Hr) | Solvent | Conversion (%) | Ratio (%) | |
|---|---|---|---|---|---|---|---|---|---|
| | | | | | | | | C17 | C18 |
| 9. | $Ti_3C_2$ | MX-09 | 280 | 30 | 15 | None | 76.43 | 25.89 | 28.90 |

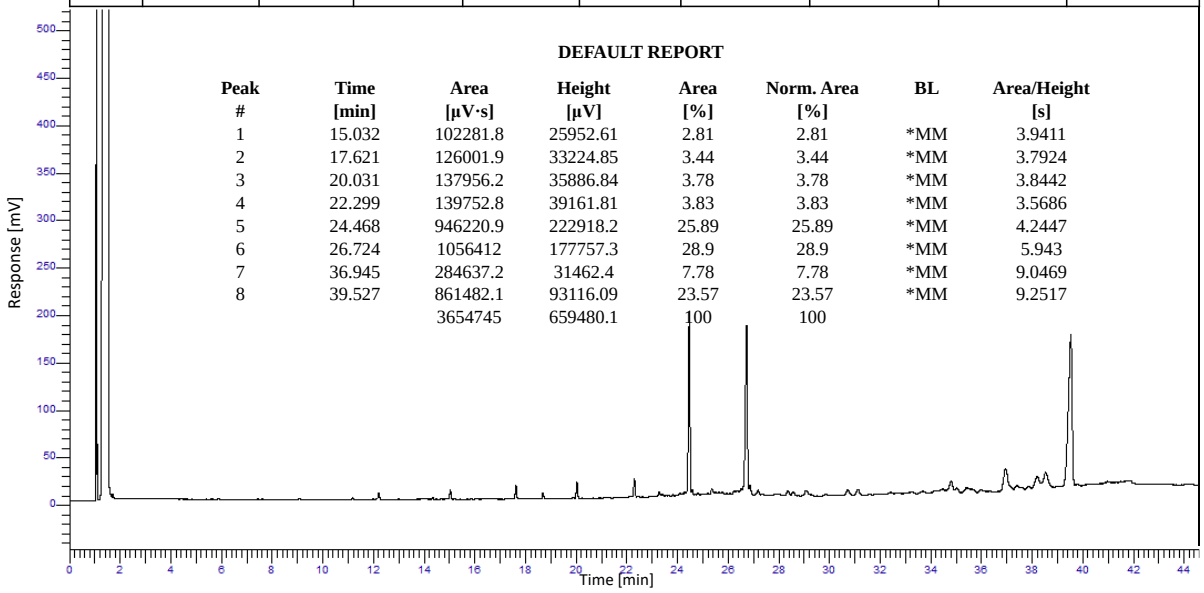


**Figure S17:** GC chromatogram for biodiesel product over $Ti_3C_2T_x$ catalyst (MX-09).

| Entry | Reaction | Code for graphs | Temp.(°C) | Pressure(B) | Time(Hr) | Solvent | Conversion (%) | Ratio (%) | |
|---|---|---|---|---|---|---|---|---|---|
| | | | | | | | | C17 | C18 |
| 10. | $Ti_3C_2$ | MX-10 | 280 | 40 | 15 | None | 98 | 40.7 | 42.52 |

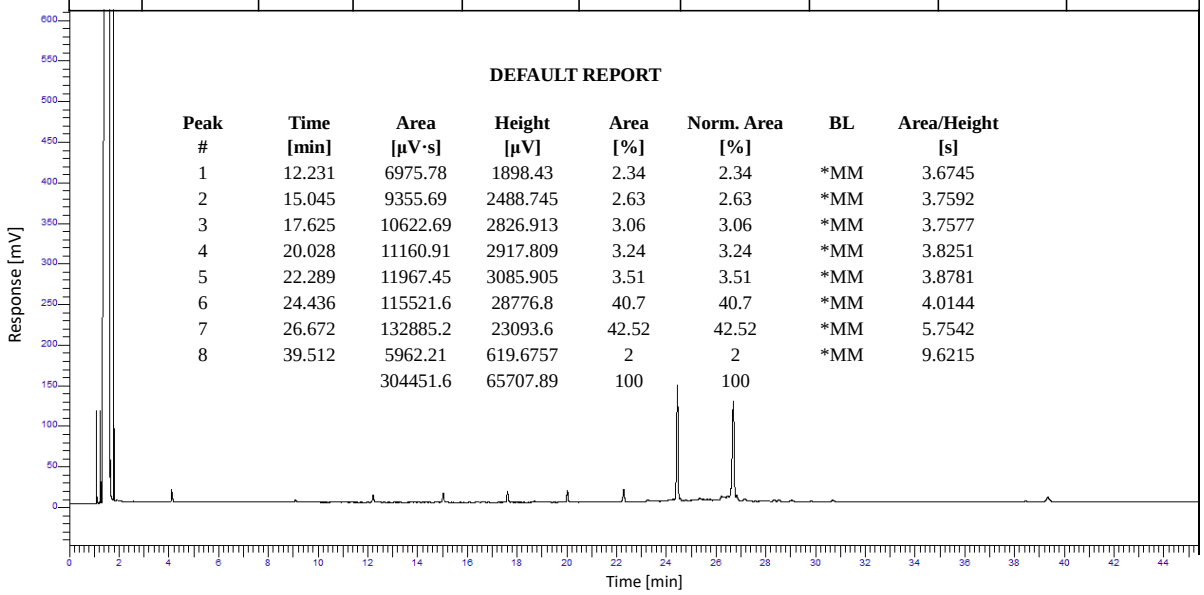


**Figure S18:** GC chromatogram for biodiesel product over $Ti_3C_2T_x$ catalyst (MX-10).

| Entry | Reaction | Code for graphs | Temp.(°C) | Pressure(B) | Time(Hr) | Solvent | Conversion (%) | Ratio (%) | |
|---|---|---|---|---|---|---|---|---|---|
| | | | | | | | | C17 | C18 |
| 11. | $Ti_3C_2$ | MX-11 | 300 | 40 | 15 | None | 100 | 43.83 | 52.17 |

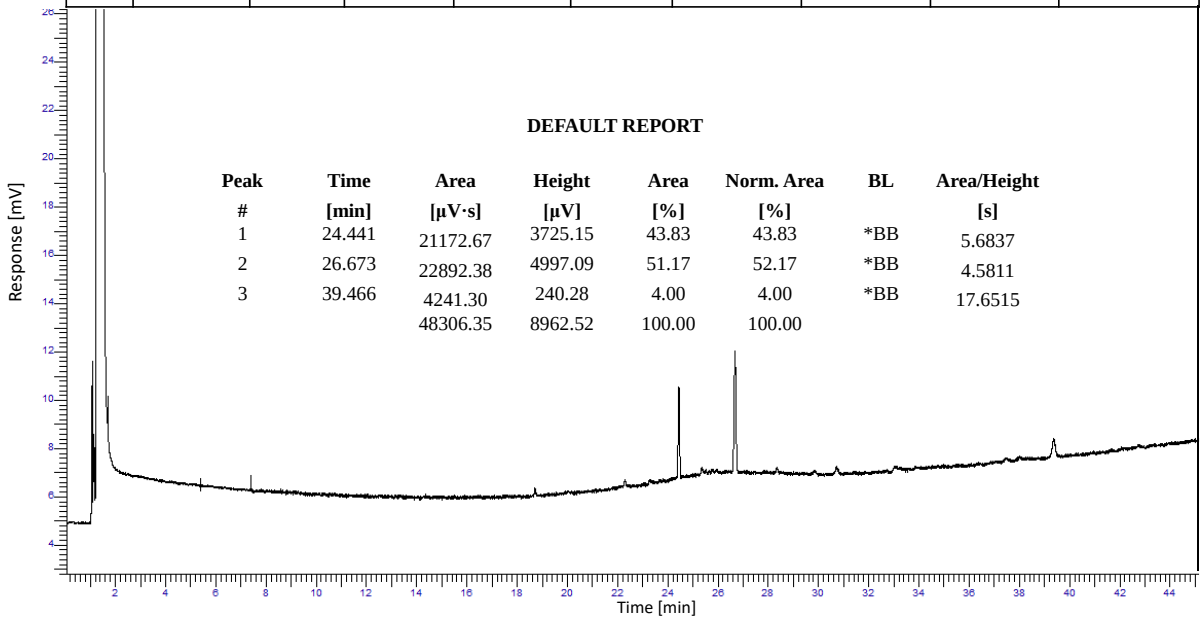


**Figure S19:** GC chromatogram for biodiesel product over $Ti_3C_2T_x$ catalyst (MX-11).

| Entry | Reaction | Code for graphs | Temp.(°C) | Pressure(B) | Time(Hr) | Solvent | Conversion (%) | Ratio (%) | |
|---|---|---|---|---|---|---|---|---|---|
| | | | | | | | | C17 | C18 |
| 12. | $Ti_3C_2$ | MX-12 | 300 | 30 | 15 | None | 100 | 61.32 | 33.37 |

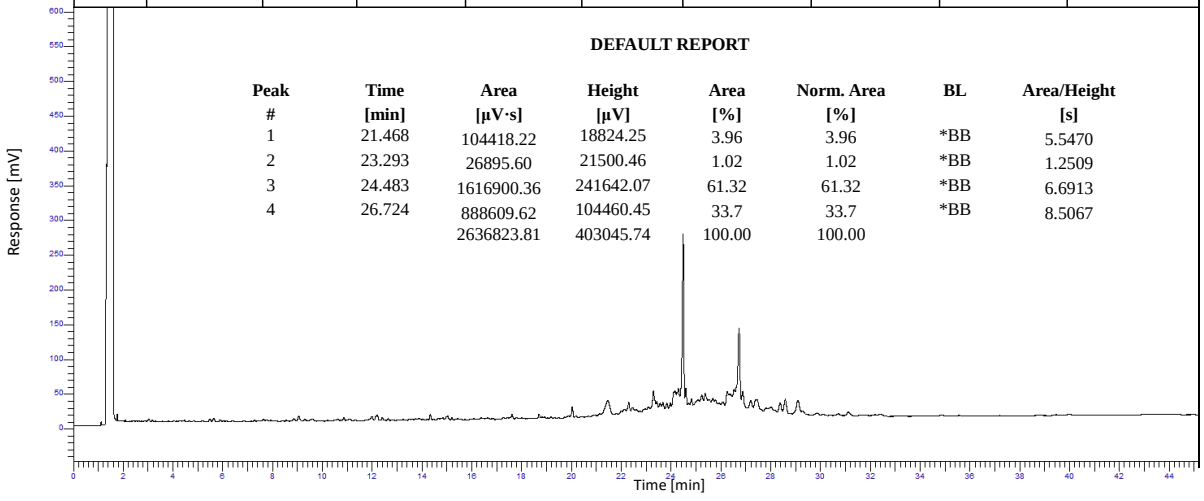


**Figure S20:** GC chromatogram for biodiesel product over $Ti_3C_2T_x$ catalyst (MX-12).

| Entry | Reaction | Code for graphs | Temp.(°C) | Pressure(B) | Time(Hr) | Solvent | Conversion (%) | Ratio (%) | |
|---|---|---|---|---|---|---|---|---|---|
| | | | | | | | | C17 | C18 |
| 13. | $Ti_3C_2$ | MX-13 | 300 | 25 | 15 | None | 100 | 66.59 | 33.41 |

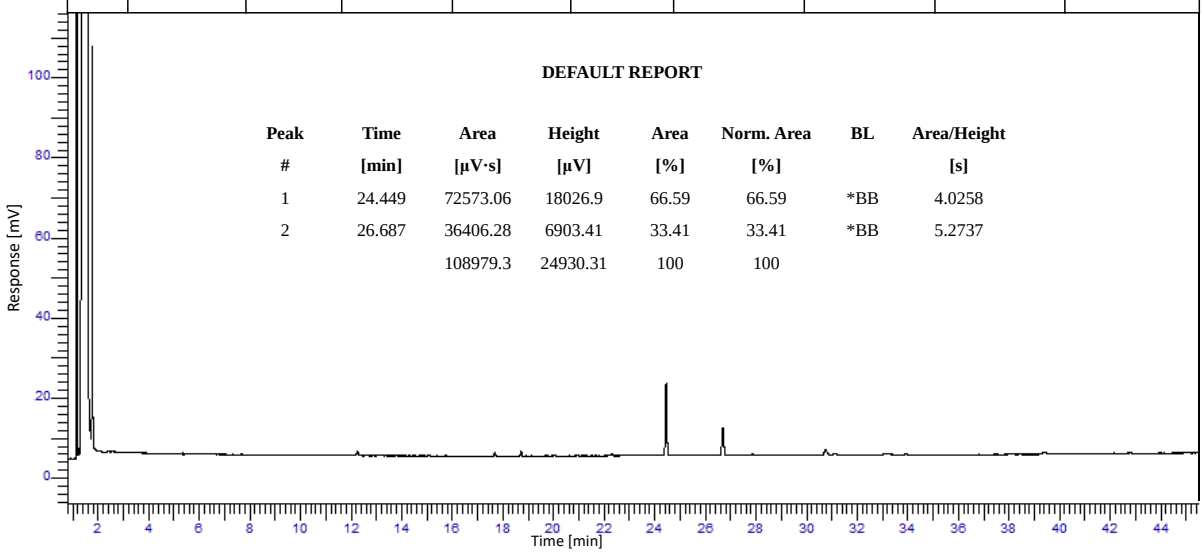


**Figure S21:** GC chromatogram for biodiesel product over $Ti_3C_2T_x$ catalyst (MX-13).

| Entry | Reaction | Code for graphs | Temp.(°C) | Pressure(B) | Time(Hr) | Solvent | Conversion (%) | Ratio (%) | |
|---|---|---|---|---|---|---|---|---|---|
| | | | | | | | | C17 | C18 |
| 14. | $Ti_3C_2$ | MX-14 | 300 | 10 | 15 | None | 72.60 | 25.46 | 21.32 |

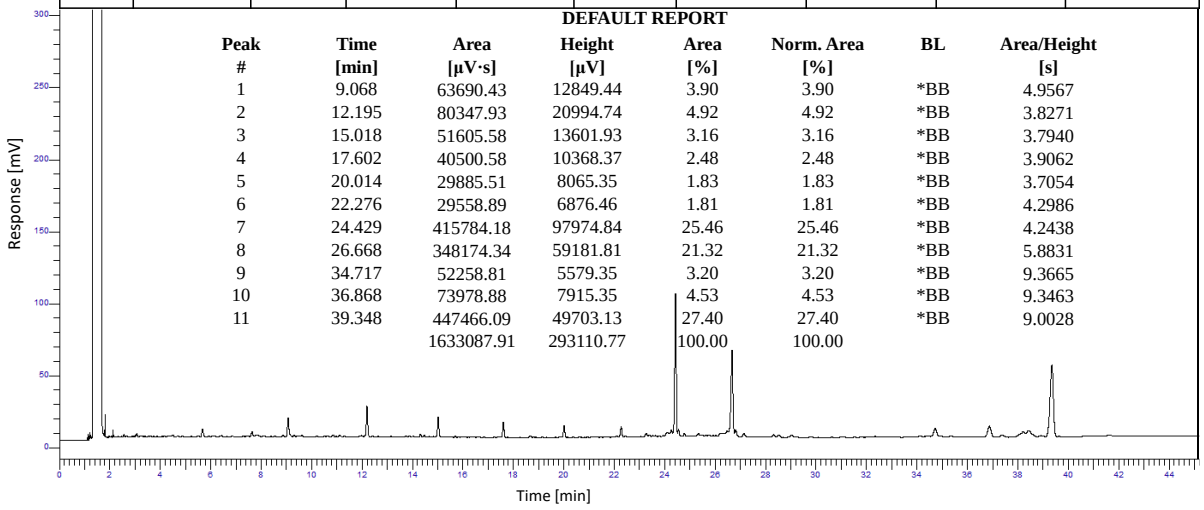


**Figure S22:** GC chromatogram for biodiesel product over $Ti_3C_2T_x$ catalyst (MX-14).

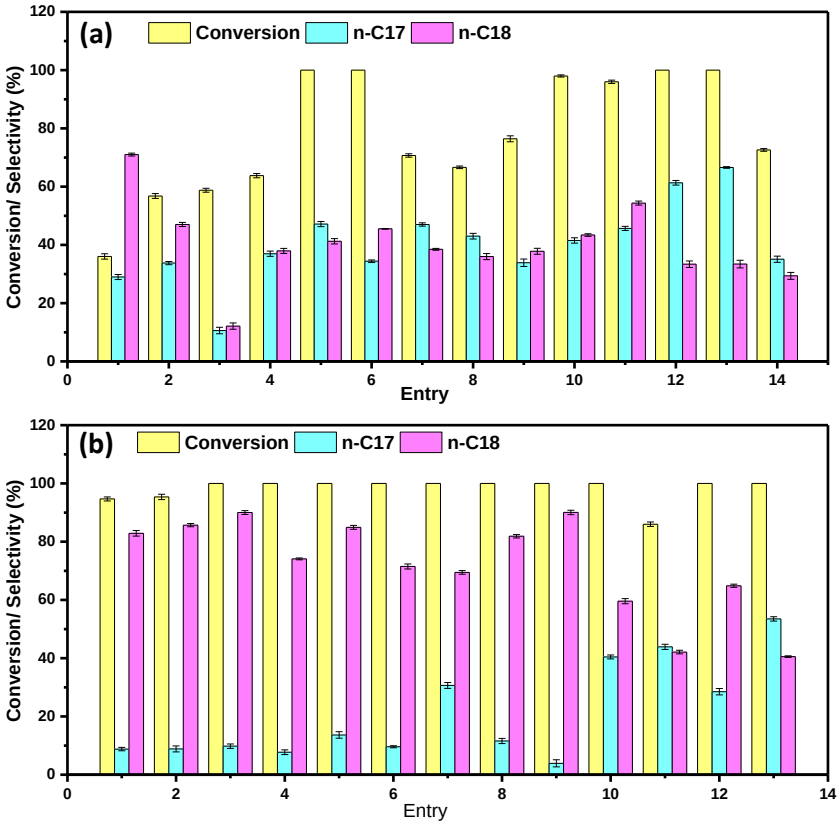


**Figure S23:** Conversation and selectivity of the methyl oleate using (a) MXene and (b) ZnO-MXene catalysts. The error bar representing the relative deviation is within 1.5%.

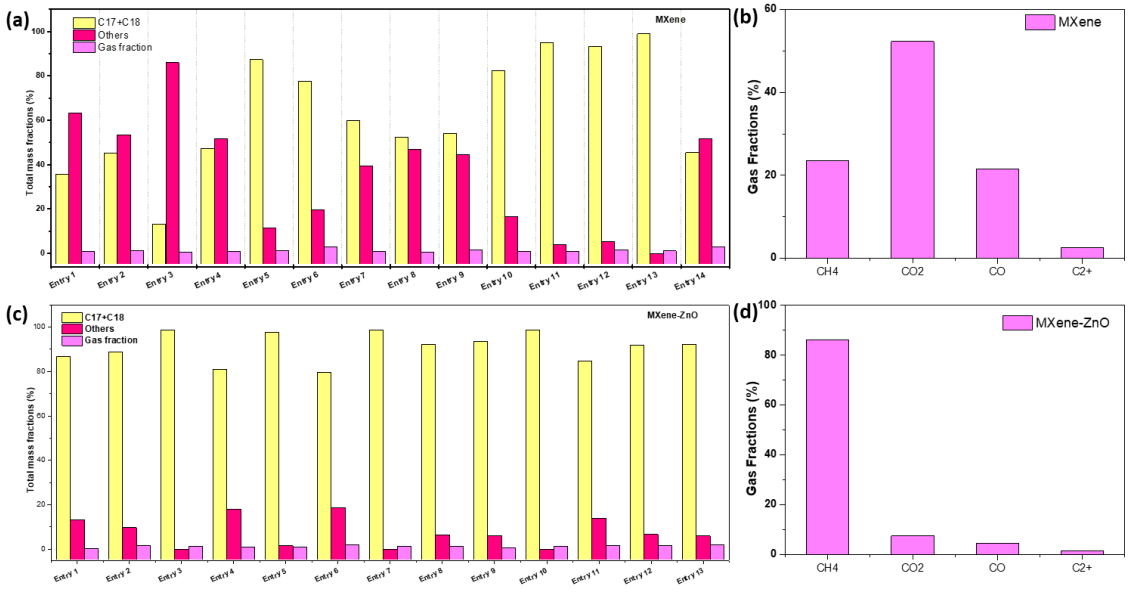


**Figure S24:** (a&c) The carbon balance for MXene and MXene-ZnO; (b) gas compositions using MXene catalyst (entry 13) and MXene-ZnO catalyst (entry 9).

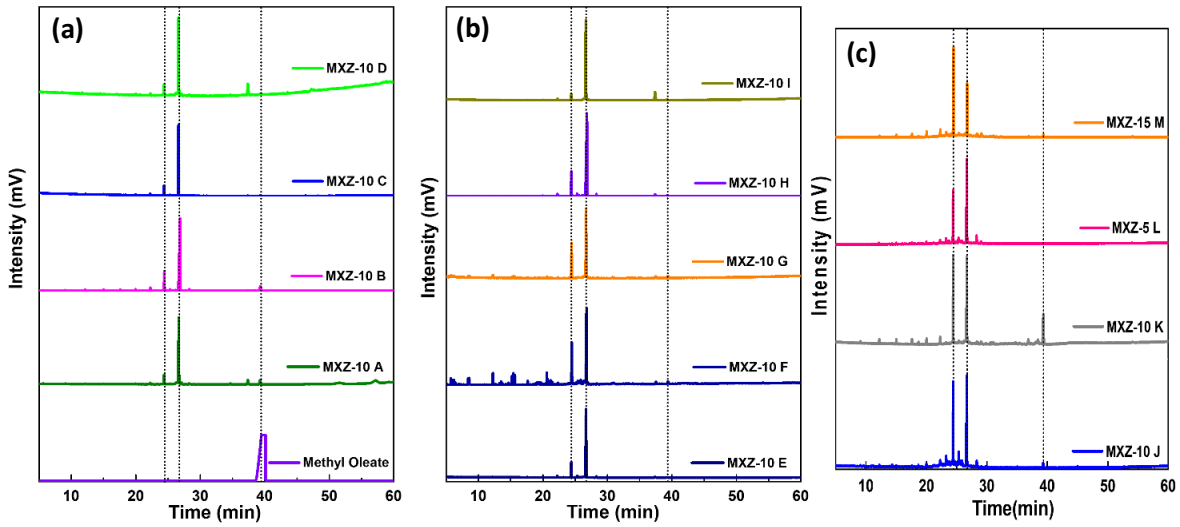


**Figure 25**. GC chromatogram of pure methyl oleate and for biodiesel product over ZnO-$Ti_3C_2T_x$ catalyst; (a) Pure Methyl Oleate and MXZ-10 A to MXZ-10D, (b) reactions from MXZ-10 to MXZ-10I, (c) reactions from MXZ-10J to MXZ-15 M.

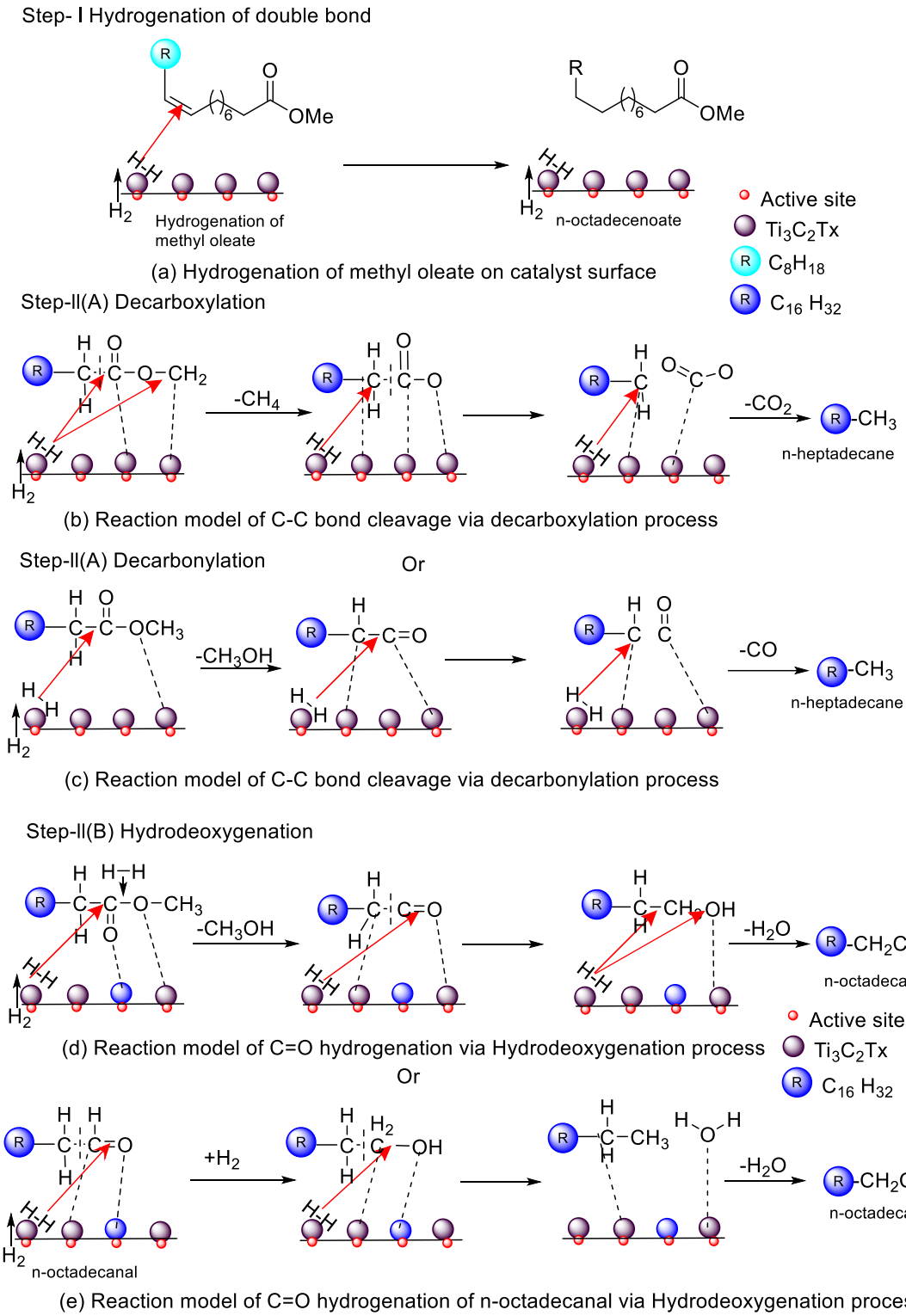


**Figure S26:** The possible reaction mechanism of selective hydrogenation of methyl oleate over MXene and MXene-ZnO.

| Entry | Reaction | Code for graphs | Temp.(°C) | Pressure(B) | Time(Hr) | Solvent | Conversion (%) | Ratio (%) | |
|---|---|---|---|---|---|---|---|---|---|
| | | | | | | | | C17 | C18 |
| 1. | ZnO-$Ti_3C_2$-10 | MXZ-10 A | 250 | 25 | 15 | None | 94.68 | 8.32 | 78.45 |

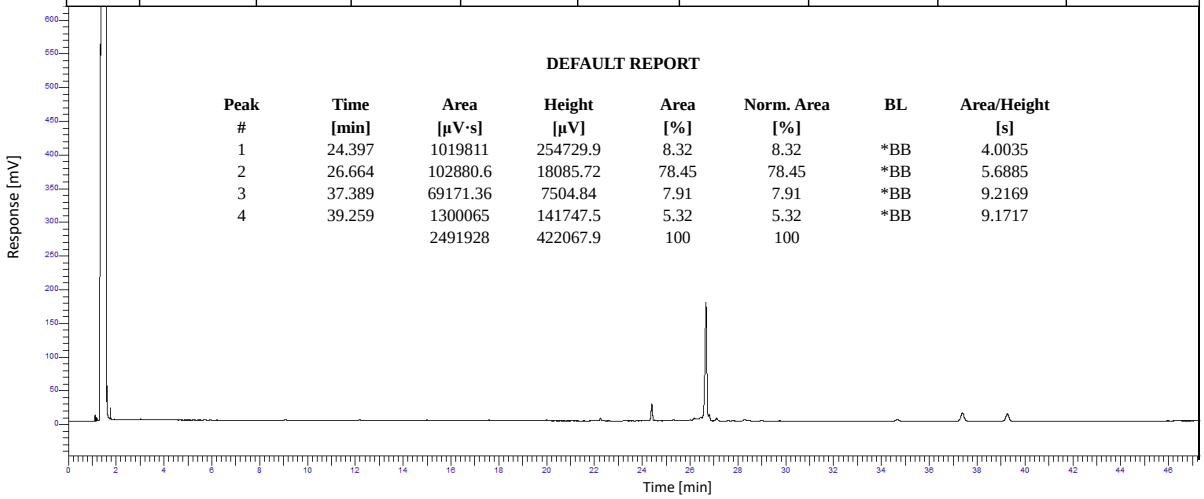


**Figure S27:** GC chromatogram for biodiesel product over ZnO-$Ti_3C_2T_x$ catalyst (MXZ-10 A).

| Entry | Reaction | Code for graphs | Temp.(°C) | Pressure(B) | Time(Hr) | Solvent | Conversion (%) | Ratio (%) | |
|---|---|---|---|---|---|---|---|---|---|
| | | | | | | | | C17 | C18 |
| 2. | ZnO-$Ti_3C_2$-10 | MXZ-10 B | 270 | 25 | 15 | None | 95.38 | 8.44 | 81.72 |

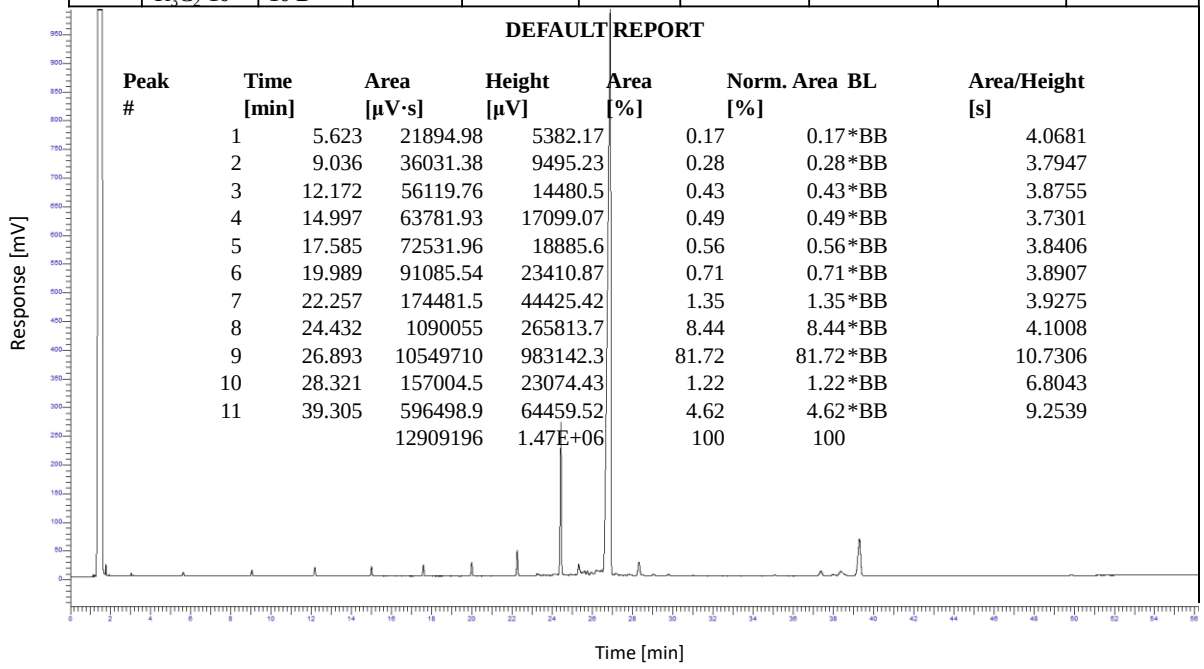


**Figure S28:** GC chromatogram for biodiesel product over ZnO-$Ti_3C_2T_x$ catalyst (MXZ-10 B).

| Entry | Reaction | Code for graphs | Temp.(°C) | Pressure(B) | Time(Hr) | Solvent | Conversion (%) | Ratio (%) | |
|---|---|---|---|---|---|---|---|---|---|
| | | | | | | | | C17 | C18 |
| 3. | ZnO-$Ti_3C_2$-10 | MXZ-10 C | 280 | 25 | 15 | None | 100 | 9.79 | 90.01 |

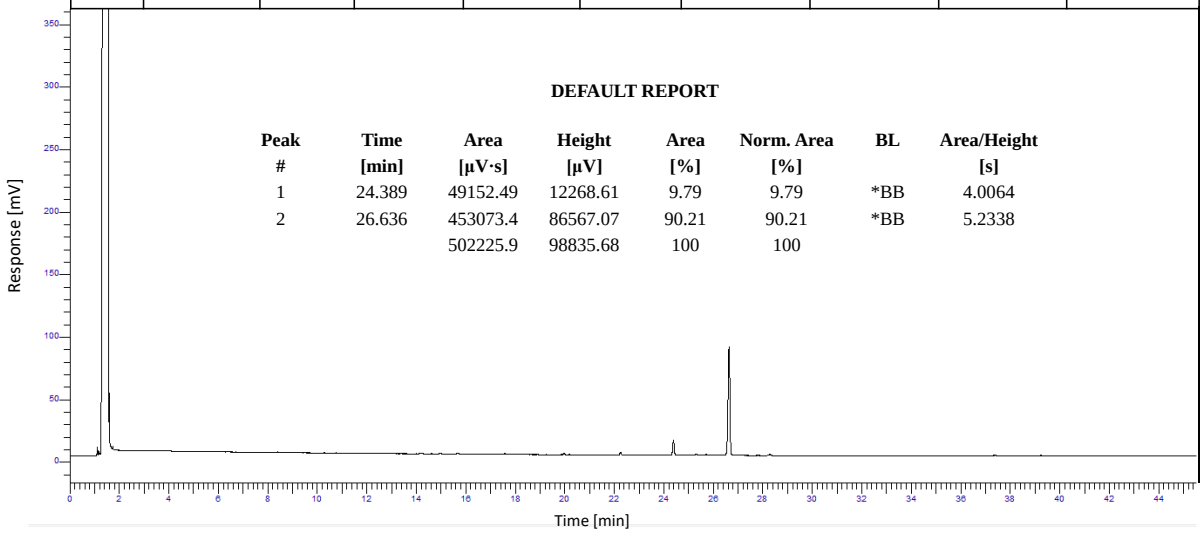


**Figure S29:** GC chromatogram for biodiesel product over ZnO-$Ti_3C_2T_x$ catalyst (MXZ-10 C).

| Entry | Reaction | Code for graphs | Temp.(°C) | Pressure(B) | Time(Hr) | Solvent | Conversion (%) | Ratio (%) | |
|---|---|---|---|---|---|---|---|---|---|
| | | | | | | | | C17 | C18 |
| 4, | ZnO-$Ti_3C_2$-10 | MXZ-10 D | 280 | 20 | 15 | None | 100 | 7.71 | 74.09 |

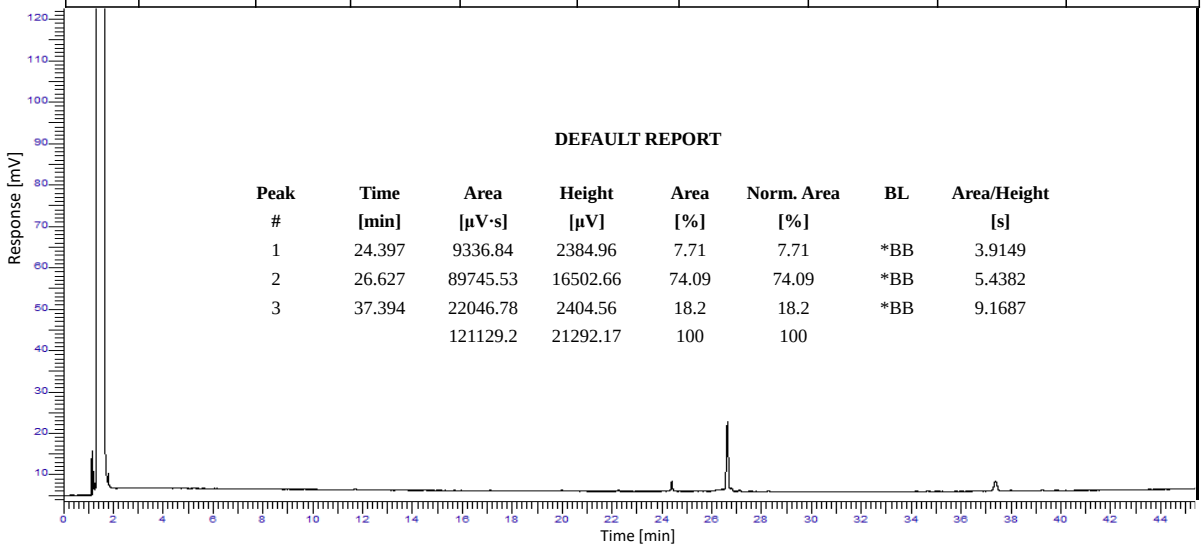


**Figure S30:** GC chromatogram for biodiesel product over ZnO-$Ti_3C_2T_x$ catalyst (MXZ-10 D).

| Entry | Reaction | Code for graphs | Temp.(°C) | Pressure(B) | Time(Hr) | Solvent | Conversion (%) | Ratio (%) | |
|---|---|---|---|---|---|---|---|---|---|
| | | | | | | | | C17 | C18 |
| 5. | ZnO-$Ti_3C_2$-10 | MXZ-10 E | 280 | 30 | 15 | None | 100 | 13.64 | 84.92 |

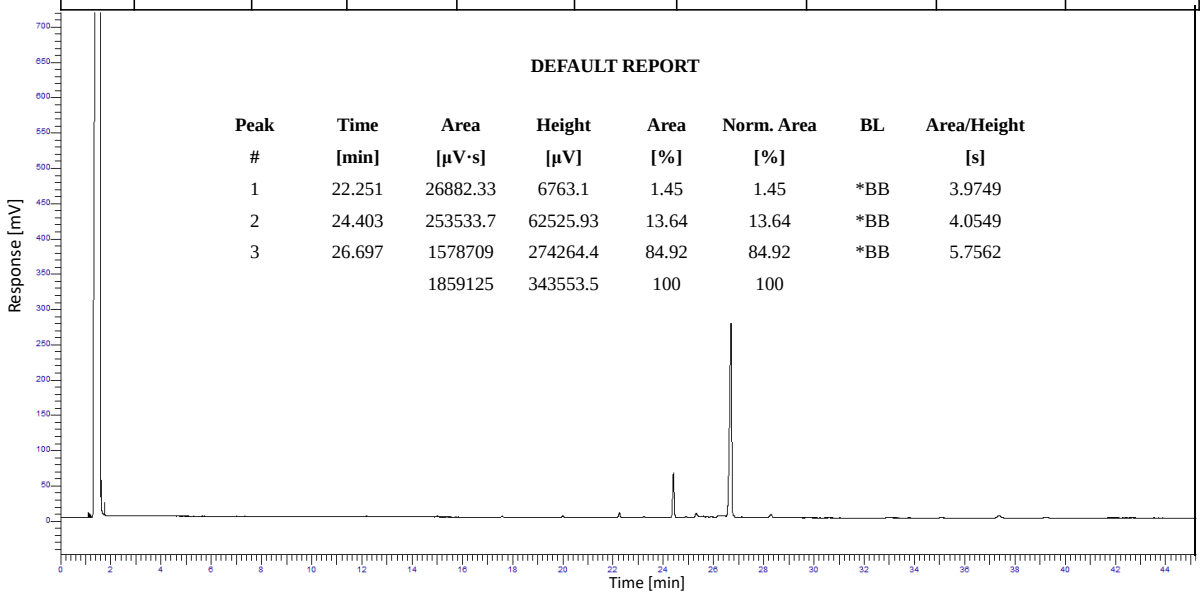


**Figure S31:** GC chromatogram for biodiesel product over ZnO-$Ti_3C_2T_x$ catalyst (MXZ-10 E).

| Entry | Reaction | Code for graphs | Temp.(°C) | Pressure(B) | Time(Hr) | Solvent | Conversion (%) | Ratio (%) | |
|---|---|---|---|---|---|---|---|---|---|
| | | | | | | | | C17 | C18 |
| 6. | ZnO-$Ti_3C_2$-10 | MXZ-10 F | 280 | 40 | 15 | None | 100 | 9.59 | 71.50 |

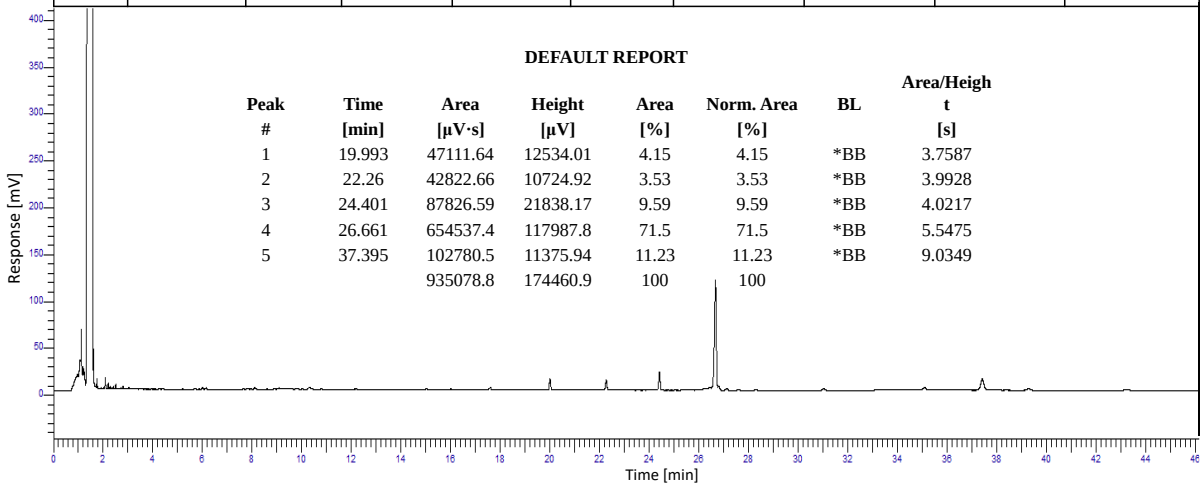


**Figure S32:** GC chromatogram for biodiesel product over ZnO-$Ti_3C_2T_x$ catalyst (MXZ-10 F).

| Entry | Reaction | Code for graphs | Temp.(°C) | Pressure(B) | Time(Hr) | Solvent | Conversion (%) | Ratio (%) | |
|---|---|---|---|---|---|---|---|---|---|
| | | | | | | | | C17 | C18 |
| 7. | ZnO-$Ti_3C_2$-10 | MXZ-10 G | 300 | 40 | 15 | None | 100 | 30.64 | 69.46 |

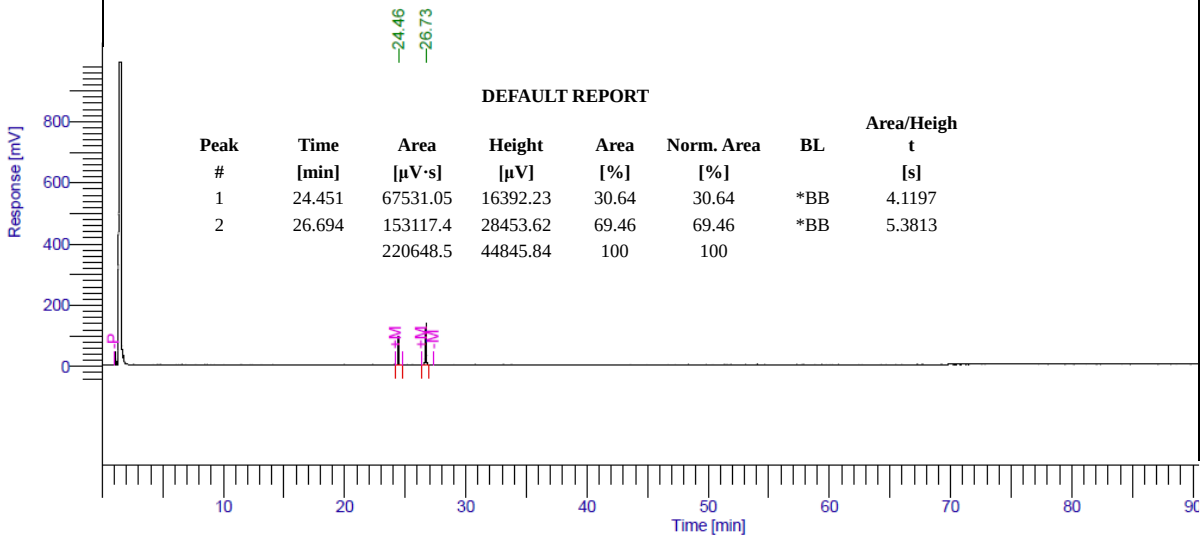


**Figure S33:** GC chromatogram for biodiesel product over ZnO-$Ti_3C_2T_x$ catalyst (MXZ-10 G).

| Entry | Reaction | Code for graphs | Temp.(°C) | Pressure(B) | Time(Hr) | Solvent | Conversion (%) | Ratio (%) | |
|---|---|---|---|---|---|---|---|---|---|
| | | | | | | | | C17 | C18 |
| 8. | ZnO-$Ti_3C_2$-10 | MXZ-10 H | 280 | 40 | 13 | None | 100 | 11.57 | 81.87 |

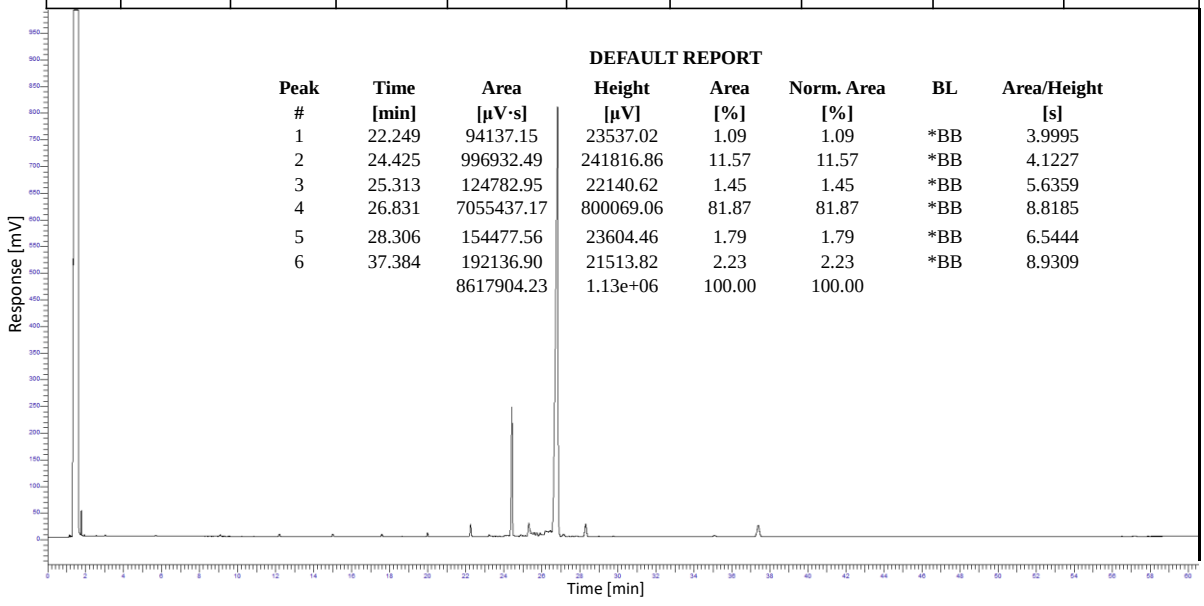


**Figure S34:** GC chromatogram for biodiesel product over ZnO-$Ti_3C_2T_x$ catalyst (MXZ-10 H).

| Entry | Reaction | Code for graphs | Temp.(°C) | Pressure(B) | Time(Hr) | Solvent | Conversion (%) | Ratio (%) | |
|---|---|---|---|---|---|---|---|---|---|
| | | | | | | | | C17 | C18 |
| 9. | ZnO-$Ti_3C_2$-10 | MXZ-10 I | 280 | 30 | 13 | None | 100 | 3.91 | 90.04 |

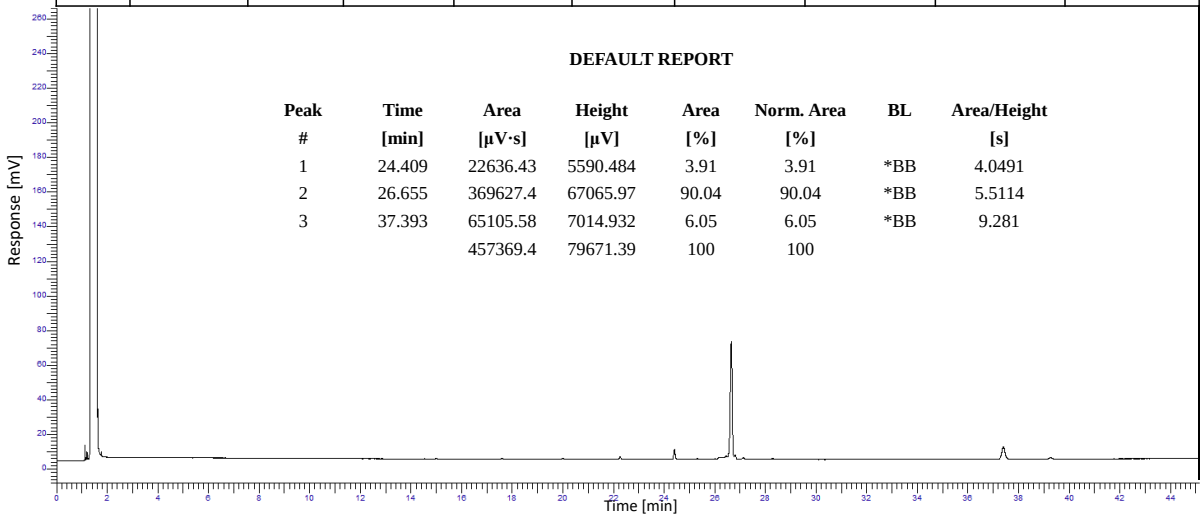


**Figure S35:** GC chromatogram for biodiesel product over ZnO-$Ti_3C_2T_x$ catalyst (MXZ-10 I).

| Entry | Reaction | Code for graphs | Temp.(°C) | Pressure(B) | Time(Hr) | Solvent | Conversion (%) | Ratio (%) | |
|---|---|---|---|---|---|---|---|---|---|
| | | | | | | | | C17 | C18 |
| 10. | ZnO-$Ti_3C_2$-10 | MXZ-10 J | 260 | 30 | 13 | None | 100 | 40.43 | 59.57 |

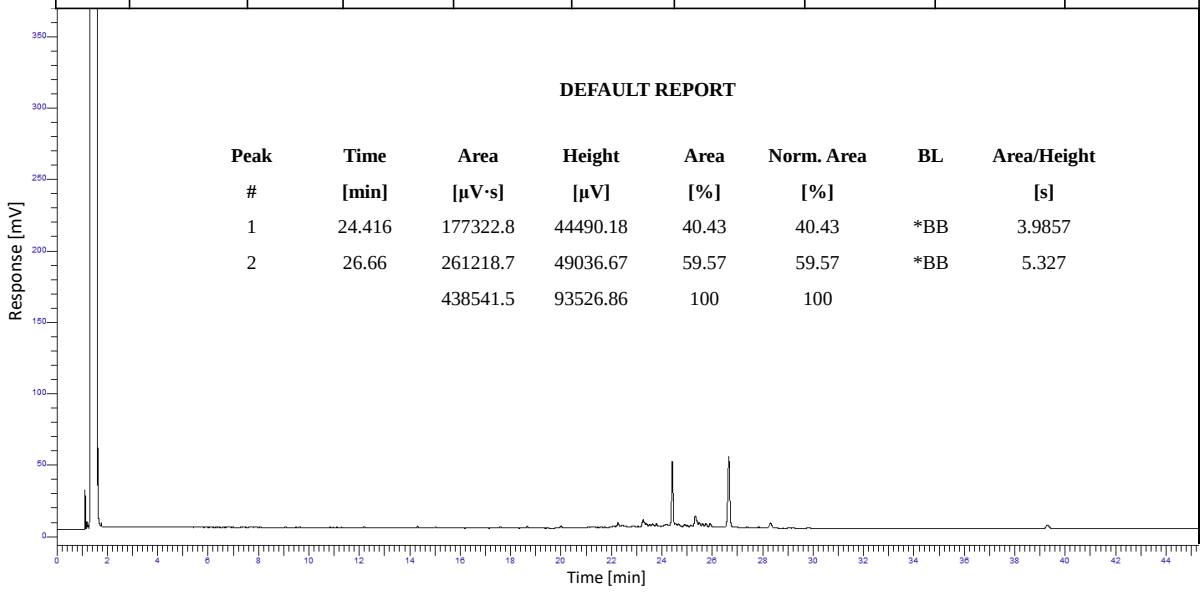


**Figure S36:** GC chromatogram for biodiesel product over ZnO-$Ti_3C_2T_x$ catalyst (MXZ-10 J).

| Entry | Reaction | Code for graphs | Temp.(°C) | Pressure(B) | Time(Hr) | Solvent | Conversion (%) | Ratio (%) | |
|---|---|---|---|---|---|---|---|---|---|
| | | | | | | | | C17 | C18 |
| 11. | ZnO-$Ti_3C_2$-10 | MXZ-10 K | 240 | 30 | 13 | None | 86 | 43.9 | 42.1 |

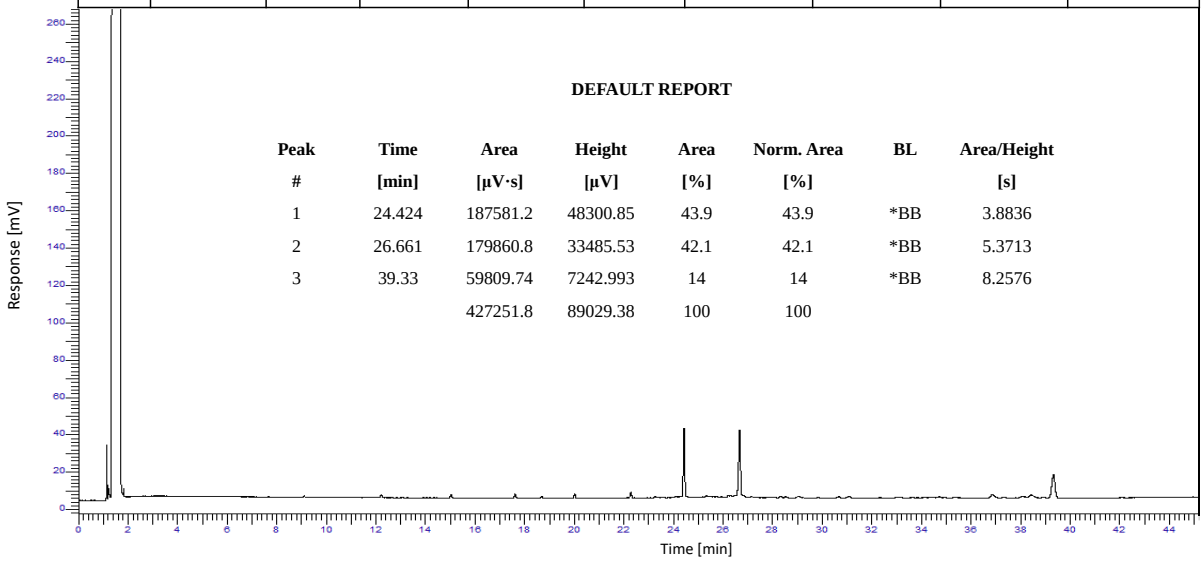


**Figure S37:** GC chromatogram for biodiesel product over ZnO-$Ti_3C_2T_x$ catalyst (MXZ-10 K).

| Entry | Reaction | Code for graphs | Temp.(°C) | Pressure(B) | Time(Hr) | Solvent | Conversion (%) | Ratio (%) | |
|---|---|---|---|---|---|---|---|---|---|
| | | | | | | | | C17 | C18 |
| 12. | ZnO-$Ti_3C_2$-10 | MXZ-5 L | 280 | 30 | 13 | None | 100 | 28.49 | 64.86 |

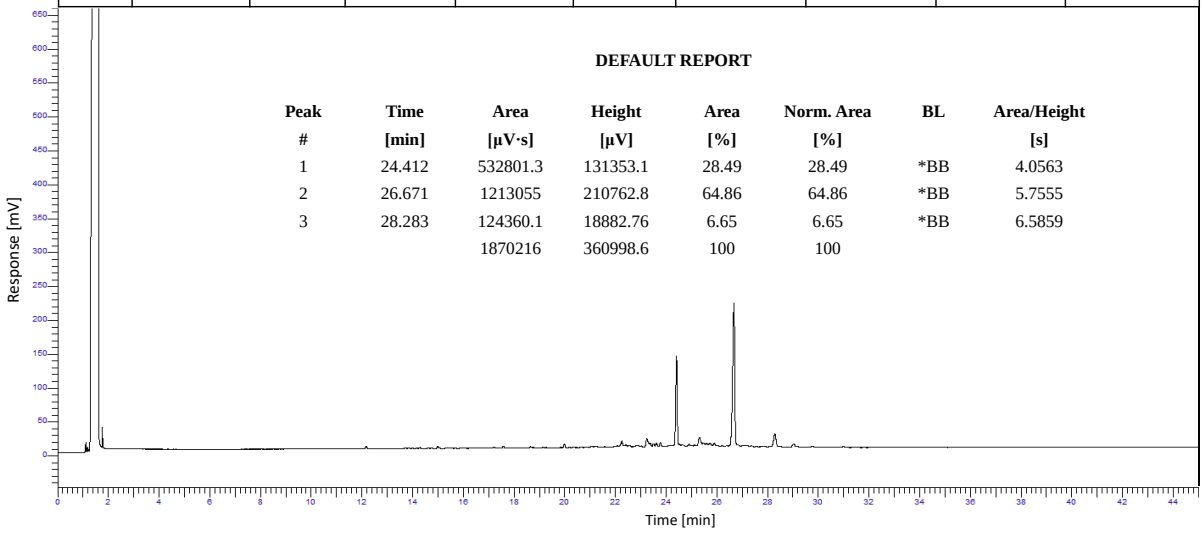


**Figure S38:** GC chromatogram for biodiesel product over ZnO-$Ti_3C_2T_x$ catalyst (MXZ-5 L).

| Entry | Reaction | Code for graphs | Temp.(°C) | Pressure(B) | Time(Hr) | Solvent | Conversion (%) | Ratio (%) | |
|---|---|---|---|---|---|---|---|---|---|
| | | | | | | | | C17 | C18 |
| 13. | ZnO-$Ti_3C_2$-10 | MXZ-15 M | 280 | 30 | 13 | None | 100 | 53.50 | 40.54 |

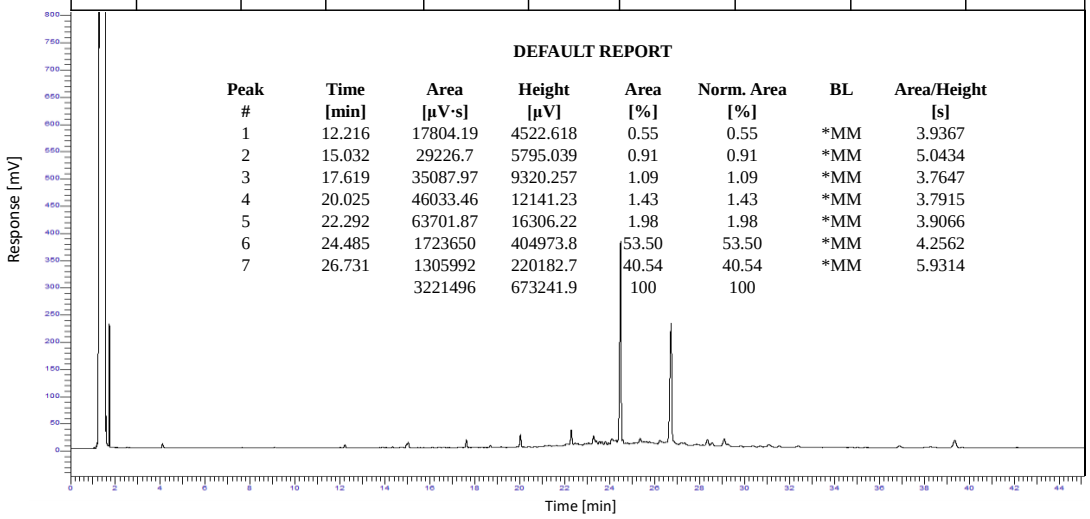


**Figure S39:** GC chromatogram for biodiesel product over ZnO-$Ti_3C_2T_x$ catalyst (MXZ-15 M).

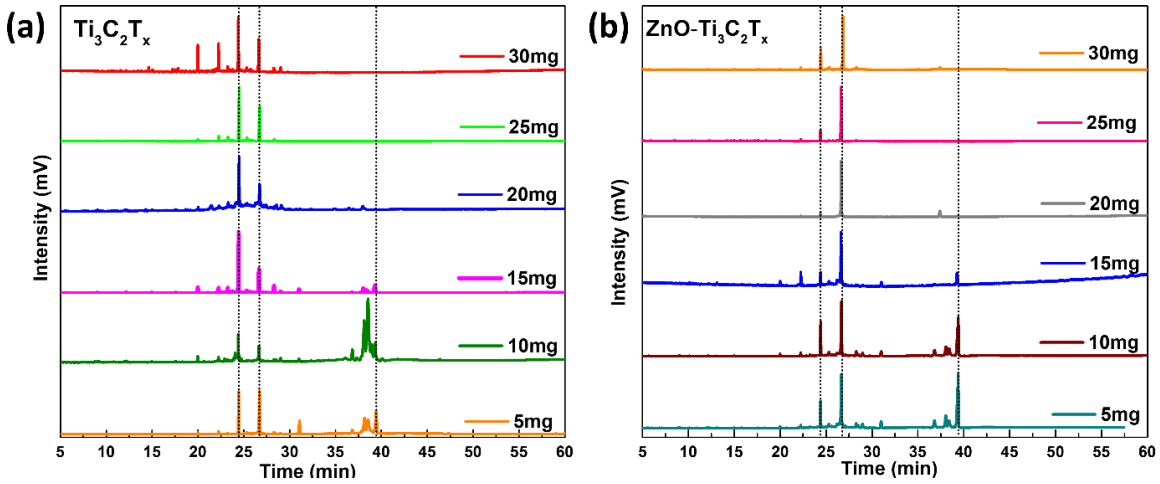


**Figure S40.** (a and b) GC chromatogram of $Ti_3C_2T_x$ and ZnO-$Ti_3C_2T_x$ with variable catalyst loading.

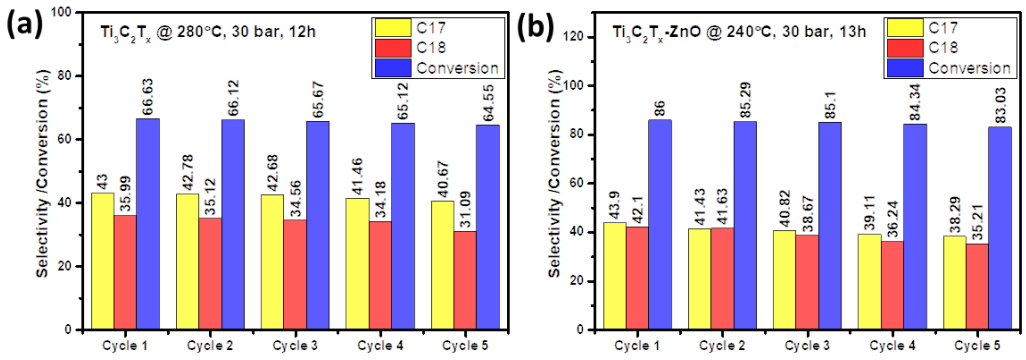


**Figure S41.** Conversion and selectivity of (a) $Ti_3C_2T_x$ and (b) ZnO-$Ti_3C_2T_x$ up to 5 cycles at lower conversion reactions.

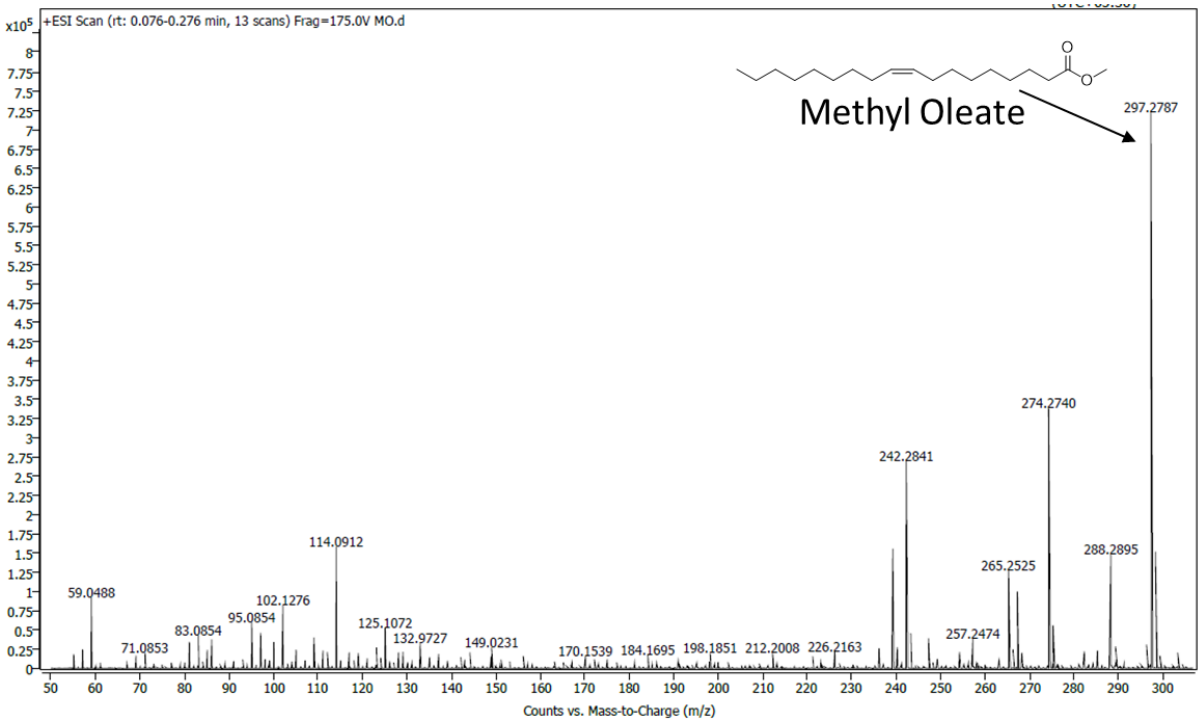


**Figure S42:** HRMS spectrum of pure methyl oleate (m/z 297.2787).

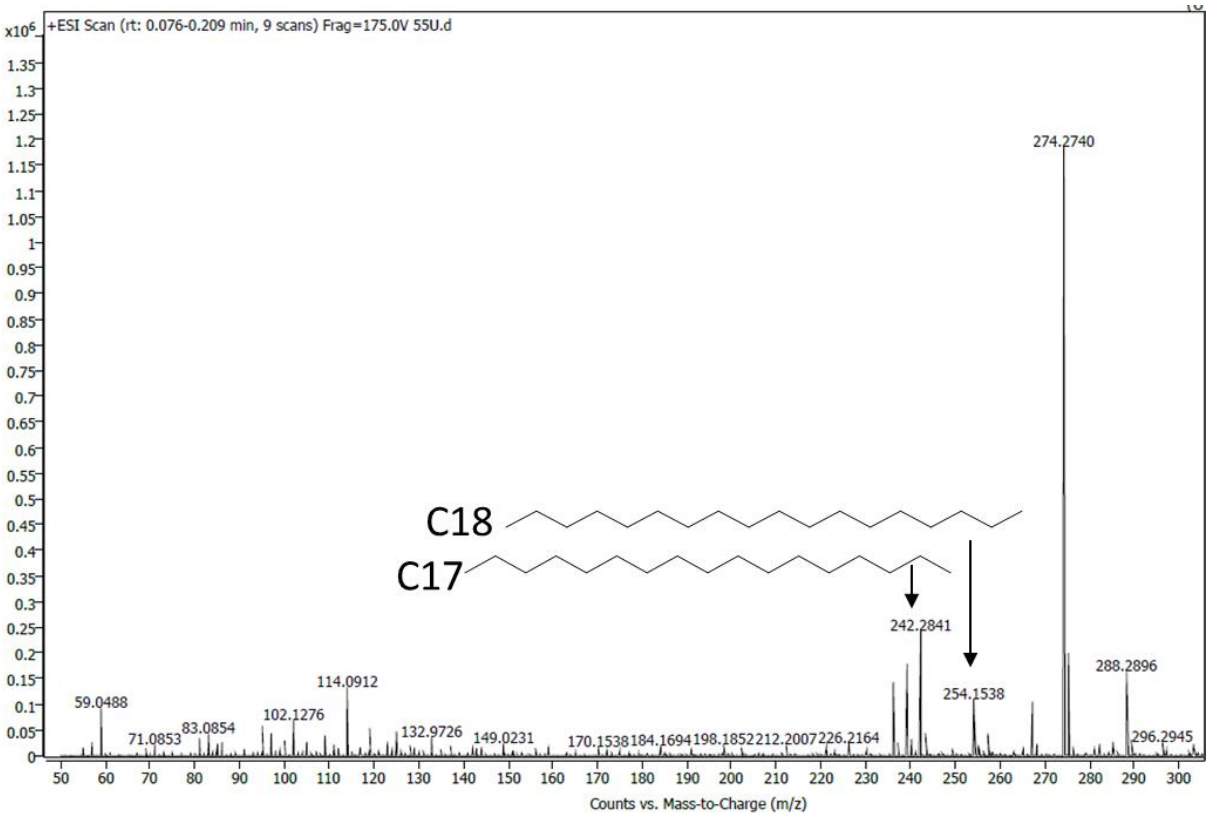


**Figure S43:** HRMS spectrum of reaction after hydrotreatment process using MXZ-10 catalyst (m/z of C18 (254.1538 and C17 (242.2841).

**$^{1}$H NMR spectrum**

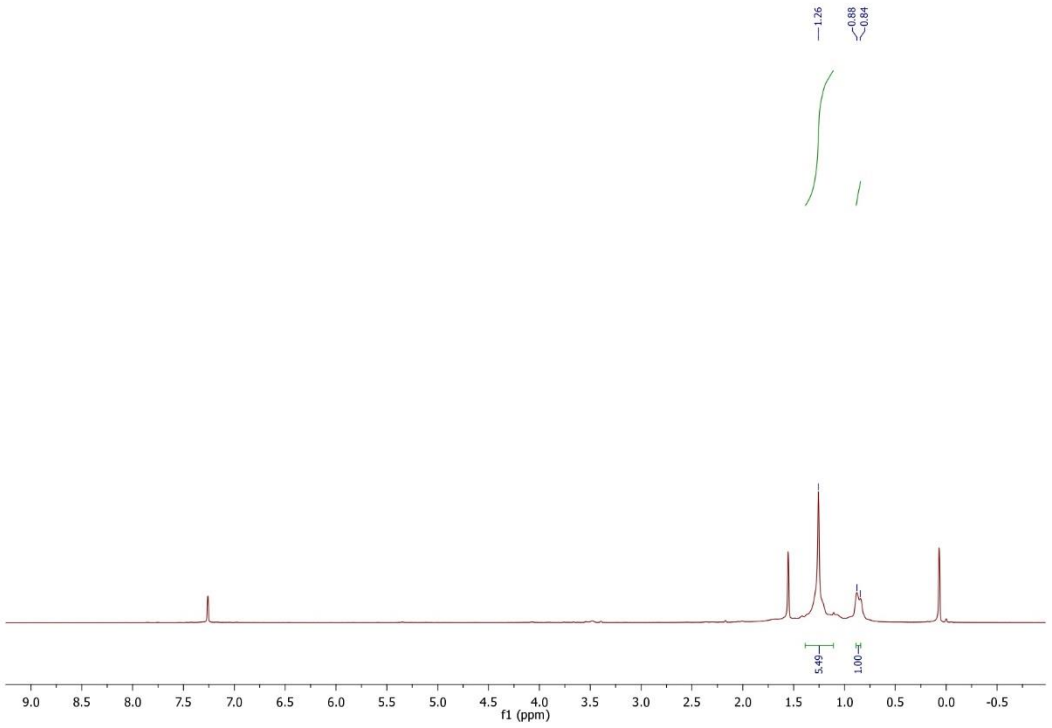


**Figure S44:** $^{13}$C NMR of hydrotreatment reaction

**$^{13}$C NMR spectrum**

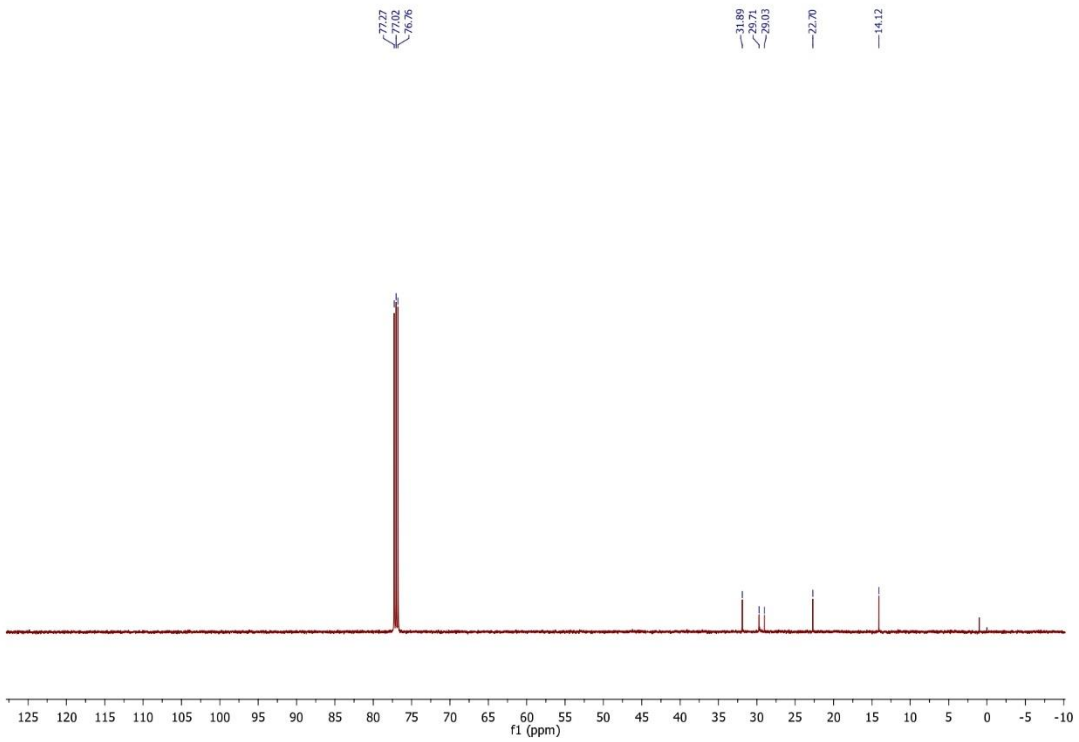

**Figure S45:** $^{13}C$ NMR of hydrotreatment reaction.

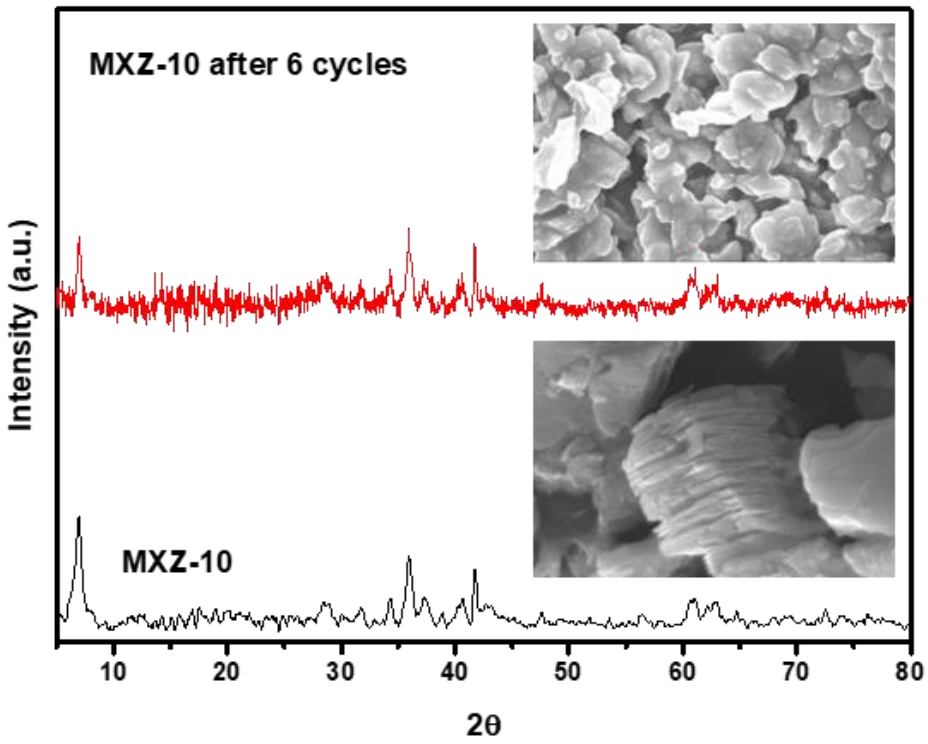


**Figure S46:** XRD of fresh catalyst and reused catalyst of MXZ-10 with SEM images.

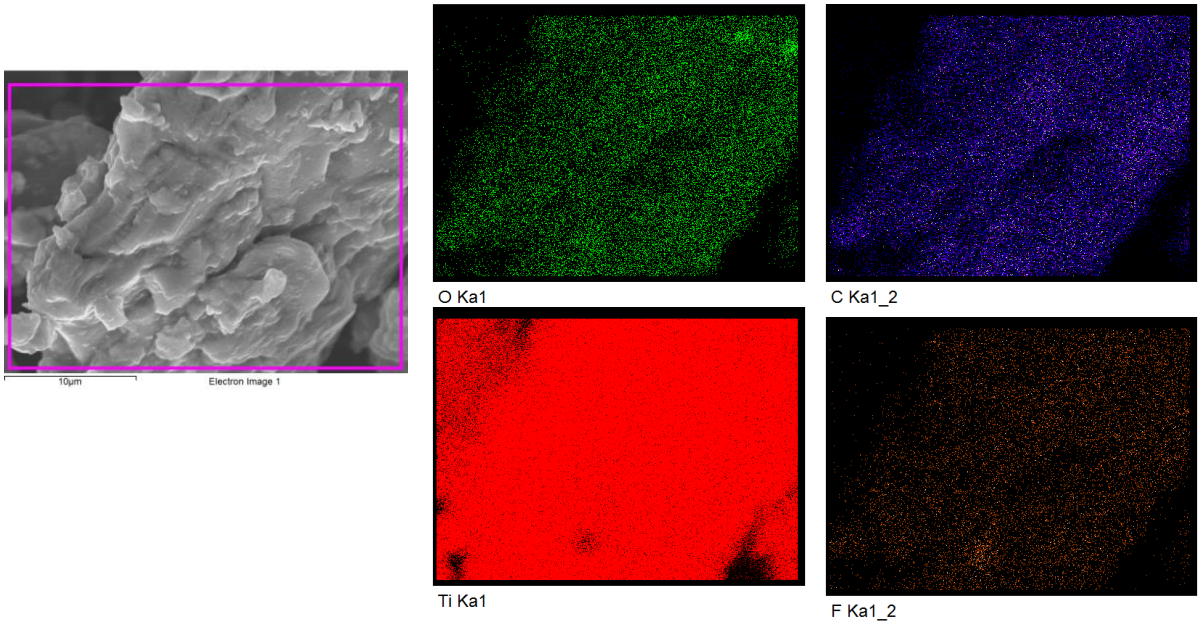


**Figure S47:** SEM image and EDX elemental mapping after the hydrotreatment process of $Ti_3C_2T_x$.

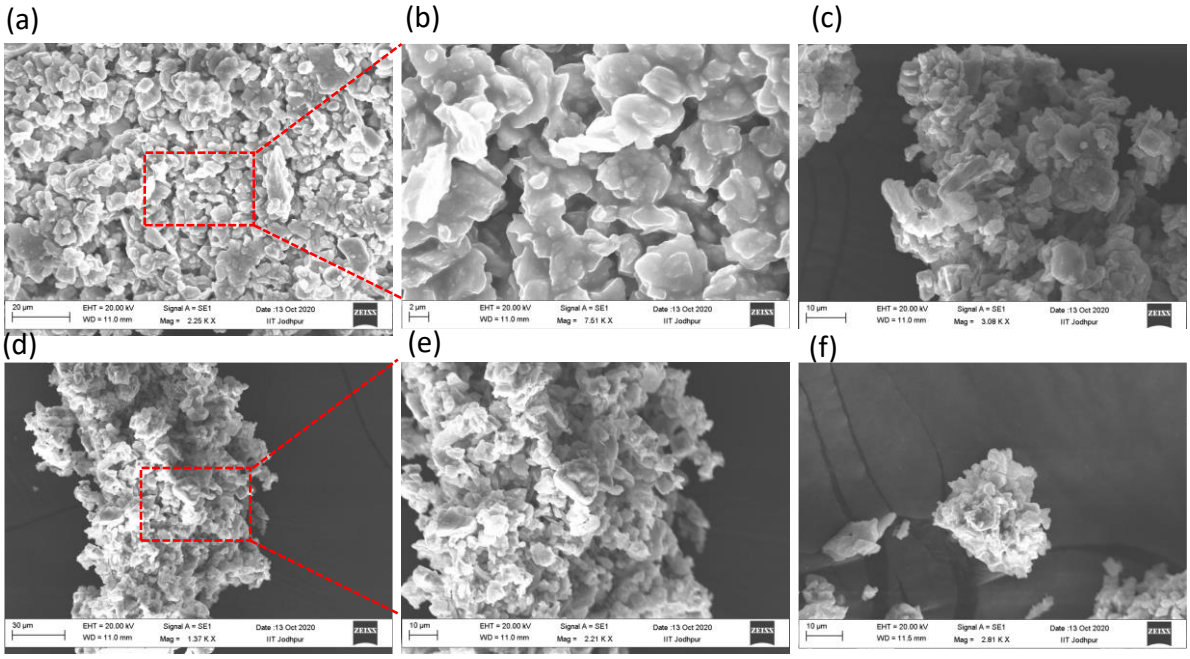


**Figure S48:** SEM image of $Ti_3C_2T_x$, after hydrotreatment reaction at different reaction condition.

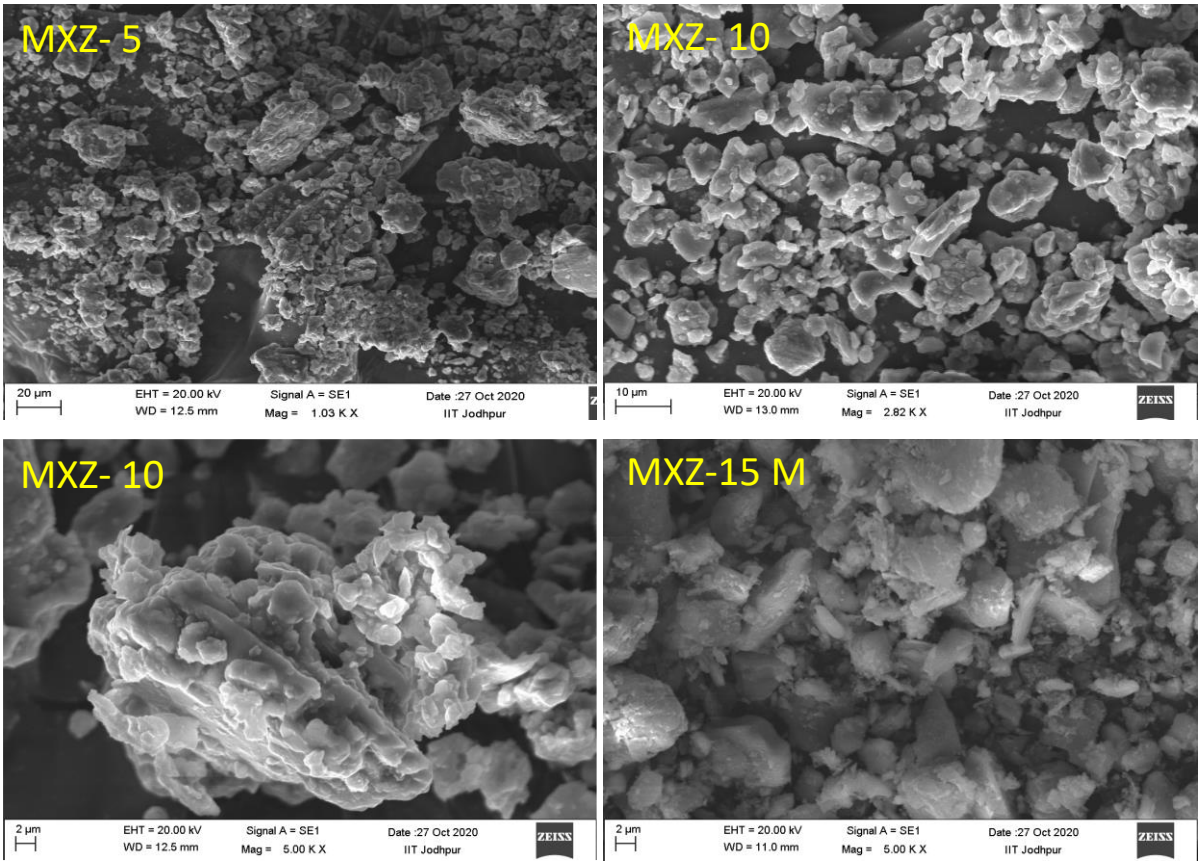


**Figure S49:** SEM image of ZnO-$Ti_3C_2T_x$ catalyst after hydrotreatment reaction at different reaction condition.

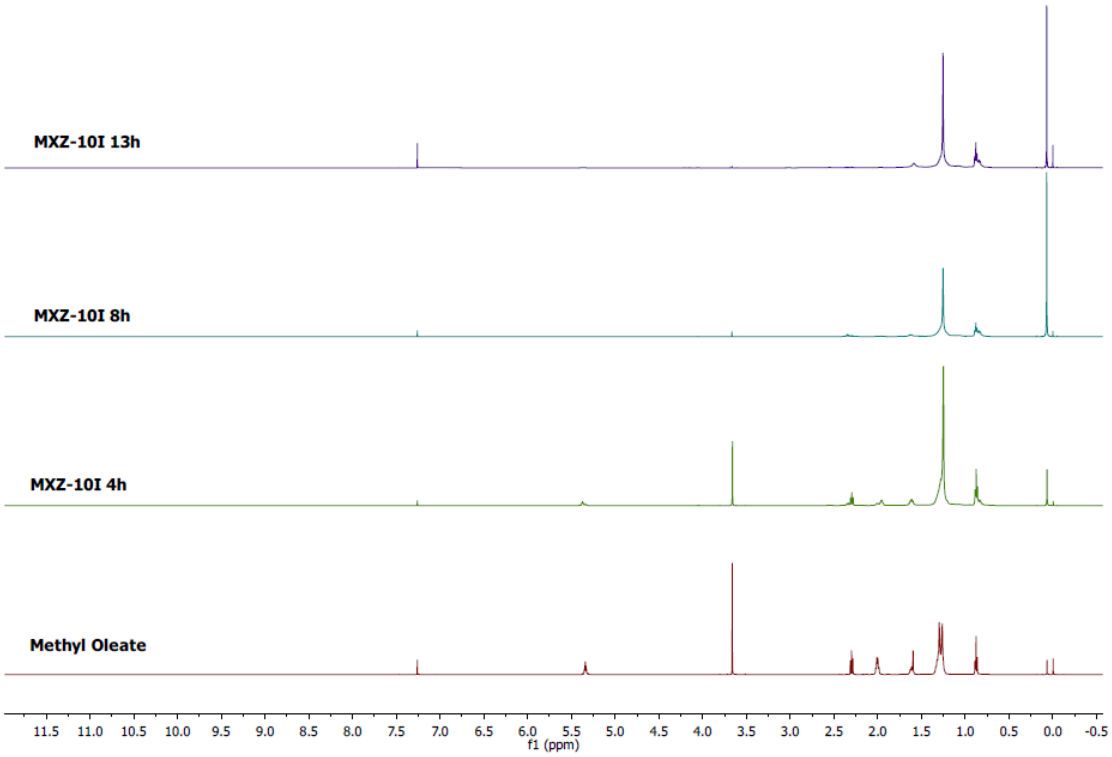


**Figure S50:** (a) $^{1}$H NMR of hydrotreatment reaction with time-dependent study.

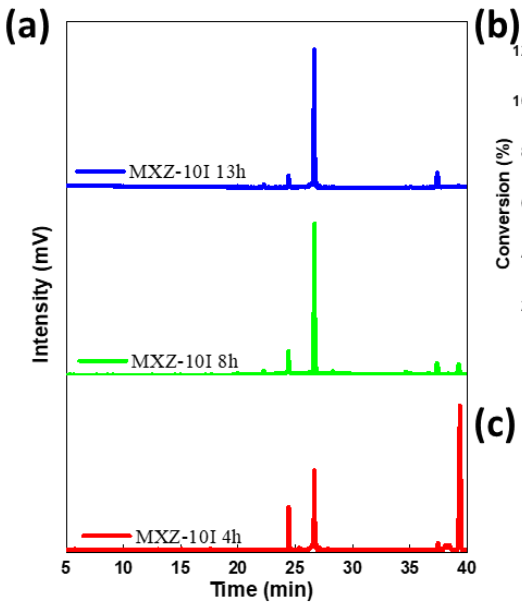


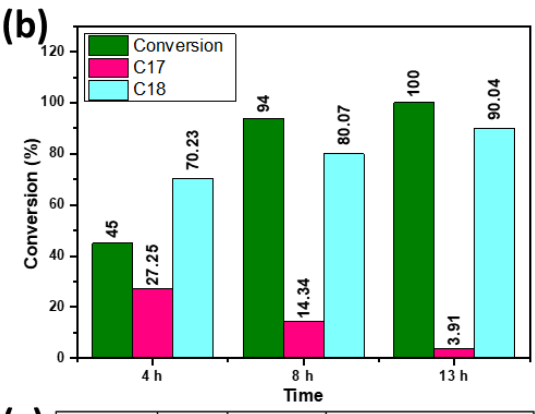


(c)

| Entry | Time (h) | Conversion (%) | Selectivity (%) | |
|---|---|---|---|---|
| | | | n-C17 | n-C18 |
| 1. | 4 | 45 | 27.25 | 70.23 |
| 2. | 8 | 94 | 14.34 | 80.07 |
| 3. | 13 | 100 | 3.91 | 90.04 |

**Figure S51:** (a) GC chromatogram of hydrotreatment reaction with time-dependent study; (b-c) Conversation and selectivity data of Entry 9 at 4, 8 and 13h.

| Catalyst | Metal loaded | Substrate | Solvent | Temp (°C) | Pressure (bar) | Time (h) | Conversion | Selectivity | product | Ref. |
|---|---|---|---|---|---|---|---|---|---|---|
| **MXene-nano sheet** | - | Guaiacol | Hexadecane-dodecane | 350 | 50 | 4 | 56 | 61 | Phenol | [1] |
| **MXene-nano sheet** | - | Guaiacol | hexadecane dodecane | 350 | 50 | 4 | 56 | 17 | methylanisole | [1] |
| **Ti-based MXene** | - | furfural | 2-propanol | 180 | 5 | 48 | 62 | 49 | Furfuryl alcohol | [2] |
| **MXene** | Ni | Palmitic Acid | decane | 300 | 40 | 4 | 100 | 78.11 | Alkane | [3] |
| **$MoO_2$@$Mo_2CT_x$** | Ni | Palmitic Acid | decane | 280 | 2 | 4 | 100 | 97.09 | Alkane | [3] |
| **$Ti_3C_2N$-CNT** | Co | Propyne | | 150 | 1 | 5.4 | 99 | 96 | propene | [4] |
| **$Ti_3C_2Tx$** | Pt | pchloronitrobenzene | Ethanol-water | 30 | 10 | 1 | 100 | 99.5 | p-chloroaniline | [5] |
| **$Ti_3C_2Tx$** | | Methyl Oleate | Solvent-free | 300 | 30 | 15 | 100 | 61.3 | C17 | This study |
| **$Ti_3C_2Tx$** | Zn | Methyl Oleate | Solvent-free | 280 | 30 | 13 | 100 | 90.04 | C18 | This study |

**Table S1:** Comparative study of MXene and MXene-ZnO catalyst with previously reported study.

References:

[1] E. Blanco, A. Rosenkranz, R. Espinoza-González, V.M. Fuenzalida, Z. Zhang, S. Suárez, N. Escalona, Catalytic performance of 2D-Mxene nano-sheets for the hydrodeoxygenation (HDO) of lignin-derived model compounds, Catalysis Communications 133 (2020) 105833. https://doi.org/https://doi.org/10.1016/j.catcom.2019.105833.

[2] M. Naguib, W. Tang, K.L. Browning, G.M. Veith, V. Maliekkal, M. Neurock, A. Villa, Catalytic Activity of Ti-based MXenes for the Hydrogenation of Furfural, ChemCatChem 12(22) (2020) 5733-5742. https://doi.org/https://doi.org/10.1002/cctc.202000977.

[3] J. Liang, T. Chen, J. Liu, Q. Zhang, W. Peng, Y. Li, F. Zhang, X. Fan, Chemoselective hydrodeoxygenation of palmitic acid to diesel-like hydrocarbons over Ni/$MoO_2$@$Mo_2$CTx catalyst with extraordinary synergic effect, Chemical Engineering Journal 391 (2020) 123472. https://doi.org/https://doi.org/10.1016/j.cej.2019.123472.

[4] J. Chen, M. Chu, F. Lyu, J. Gong, L. Wu, L. Liu, Y. Xu, Q. Zhang, Strong Synergy between Ti3C2 and N-Doped Co Nanoparticles Boosts the Selective Hydrogenation of Propyne, Industrial & Engineering Chemistry Research 58(47) (2019) 21413-21418. https://doi.org/10.1021/acs.iecr.9b05234.

[5] Q. Chen, W. Jiang, G. Fan, Pt nanoparticles on $Ti_3C_2$Tx-based MXenes as efficient catalysts for the selective hydrogenation of nitroaromatic compounds to amines, Dalton Transactions 49(42) (2020) 14914-14920. https://doi.org/10.1039/D0DT02594A.